



Research paper

Model predictive controller based design for energy optimization of the hybrid shipboard microgrids

Farooq Alam ^{a,b} *, Sajjad Haider Zaidi ^a , Arsalan Rehmat ^b , Bilal M. Khan ^a

^a Department of Electronics and Power Engineering (EPE), Pakistan Navy Engineering College (PNEC), National University of Sciences and Technology (NUST), Karachi, Pakistan

^b Karachi Institute of Economics and Technology (KIET), Karachi, Pakistan

ARTICLE INFO

Keywords:

Energy optimization
Hierarchical control designs
Hybrid AC/DC microgrid
Hardware implementations
Model predictive control (MPC)
Shipboard microgrids (SMGs)

ABSTRACT

Nowadays, the need for hybrid Shipboard Microgrid (SMG) optimization, integration, and control is rising constantly. This paper provides an optimal hierarchical control scheme for integrating microgrid systems comprising AC and DC electrical distribution networks for a shipboard architecture. Utilizing this power by the inverter can result in rapid spikes in the AC/DC voltages, potentially reducing the overall performance of the hybrid microgrid. The proposed Model Predictive Control (MPC) based controller shows better performances in the reduction of transient droops of the AC/DC voltages and handling parametric changes, load variations, and grid transitions. We provided the analytical solution for implementing proposed optimal design of hierarchical control for a multi-DG and renewable energy resources (RESs) integration-based shipboard microgrid. The performance of proportional integral (PI), Sliding Mode Controller (SMC), and MPC based optimal hierarchical control designs are compared through simulation test cases with various static and dynamic load conditions, both for AC and DC-type loads. Furthermore, we extended our analysis to include multiple distribution generator (DG) and RES involvements in the system to demonstrate the enhanced performance of our design against parametric variations and undesirable faulty load conditions. Additionally, the architecture incorporates multiple DG and RES to enhance system scalability and flexibility. Simulation results validated in MATLAB/Simulink show improved energy optimization and resilience across various static and dynamic load conditions. Practical hardware implementation using the NVIDIA Jetson Nano further confirms the real-time applicability of the control strategies.

1. Introduction

With the growing need for RES integration with the SMGs, extensive research is being carried out on hybrid SMGs. Since alternating current (AC) and direct current (DC) can work together, hybrid SMG can be used for more effective operations. The microgrid idea represents a paradigm shift in traditional power systems, necessitating the evaluation and advancement of numerous mathematical models and analysis tools (Yoo et al., 2019). Microgrids offer possible methods to connect RES, battery energy storage systems (BESS), and connected loads through a variety of power electronics interfaces for integrating the DGs into the utility grid. Microgrids generate electricity through various RESs, including micro-turbines, photo-voltaic (PV), and wind turbines.

These RESs sources are integrated with the BESS as well as power electronics inverters. These inverters enable synchronization, balance

of power, voltage management, and load power sharing within the system. To address these issues, a variety of control mechanisms have been proposed, and these have been included in three levels of hierarchical control design (Jianfang et al., 2015).

Incorporating shipboard microgrids into military and commercial boats is a major step forward in maritime technology. Increased energy efficiency, better resilience, less environmental impact, and substantial cost savings in which shipboard microgrids improve the marine sector. As the marine industry works toward achieving sustainable and dependable power solutions while adhering to growing environmental requirements, their usage is expected to increase (Mutarraf et al., 2018). The marine sector expects to gain greatly from implementing these innovative power technologies. Power may be distributed and managed intelligently on board using a combination of conventional engines and renewable energy resources.

* Corresponding author at: Department of Electronics and Power Engineering (EPE), Pakistan Navy Engineering College (PNEC), National University of Sciences and Technology (NUST), Karachi, Pakistan.

E-mail address: faroq.phdee19pne@student.nust.edu.pk (F. Alam).

This optimization considerably improves energy efficiency by maximizing the effectiveness of power generation and consumption. In addition, microgrids deployed within ships improve the resilience and dependability of the whole system since renewable energy resources are integrated into shipboard microgrids to lessen dependency on fossil fuels and cut down on greenhouse gas emissions. Shipboard microgrids optimize power production and distribution, cutting fuel consumption and lowering operating costs for commercial and military boats. The marine sector may especially benefit from these savings since fuel costs often make up a significant component of operational costs. Maintaining reliable sources of power is essential for naval operations (Jena and Padhy, 2020).

As a result, researchers and investigators have been working on more efficient control strategies to address the high implementation and integration of RES. Furthermore, conventional cascade linear control (CLC) methods are less able to overcome the complexities and uncertainties of RES integration, which leads to diminished power quality concerns and instability (Espina et al., 2019). There are two main classes of secondary control. The first is centralized, whereas the second is a distributed system. To collect, process, and distribute signals in centralized systems, a central controller is required, which increases the likelihood of a single point of failure. Nevertheless, the distributed type can prevent such errors because it collects data from local controllers. A distributed secondary control mechanism is likely to be implemented with the rapid development of MGs and DGs. Power flow control and management of the energy flow by microgrid when coupled with other microgrids as well as with the main grid are the primary goals of tertiary control (Zolfaghari et al., 2022; Sahoo et al., 2021).

Global energy problems are caused by the scarcity of fossil fuels and the rising energy demand is discussed in Bharatee et al. (2022). These difficulties have prompted the electric power sector to switch to a system that generates electricity from renewable sources. However, the trend toward incorporating renewable power sources raises concerns about the reliability of power system output, control, and operation owing to environmental variability. Some auxiliary systems, including battery storage units, are integrated with RES to let them function despite the weather. The hybrid energy storage system (HESS) combines many storage technologies into a single unit to address these microgrid issues.

The paper Jithin and Rajeev (2022) introduces an adaptive power management strategy (PMS). It consists of the coordination of a supercapacitor (SC), BESS, and fuel cell (FC). The control framework, VSM-T droop control, is discussed in detail. The improved IC structure facilitates steady-state and transient responses and increases power-sharing across sub-grids. The suggested technique is unusual in that it employs a single controller to implement a power management strategy based on an index calculated from regional data. In addition, the IC's active and reactive power-sharing, as well as voltage control at AC and DC sub-grids, are all enhanced by the reference generation's adaptable nature. In addition, the suggested method enhances power-sharing under both volatile and normal loads due to the adaptive nature of reference production.

A novel idea that uses a bidirectional converter to interchange power between AC and DC microgrids. The paper Hosseinzadeh and Salmasi (2015) encouraged interest in the creation of power management systems (PMSs) since it requires a supervisory control system to divide power among its many resources. In this research, we provide a resilient optimum power management system (ROPMS) for an hybrid micro-grid by solving an optimization problem to facilitate the micro-grid's power flow. Important considerations in this strategy include satisfying power demands with as much renewable energy as possible, using as little fuel as possible for the generator, maximizing battery life, and minimizing the load on the main power converter.

In a variety of industries, including thermal, chemical, and electrical networks, MPC offers online optimal resource scheduling. By using the

MPC in electrical systems, operating costs can be reduced, renewable energy sources can be used more effectively, and degradation of the energy storage systems can be reduced (Taher et al., 2021). In an isolated microgrid powered by PV generation, a hybrid storage system consisting of a battery, supercapacitor, and regenerative fuel cell is employed to assess the application of MPC for energy management (Xie et al., 2021c). Two data-driven modules have shown how a two-level hierarchical model predictive controller (HMPC) can continuously and automatically improve the output characteristics of growing microgrids equipped with hybrid energy storage. An effective MPC based voltage control and power allocation optimization strategy for BESS has been discussed in Ni et al. (2021).

The primary novelty of this research is to design an optimal hierarchical control architecture specifically for shipboard microgrid applications. While hierarchical control has been applied in various contexts, its application within the unique setting of shipboard microgrids with their diverse energy sources, loads, and dynamic operating conditions is a novel approach. This hierarchical structure enables more robust and efficient control, addressing the complex and dynamic nature of shipboard power systems.

1. Novel Hierarchical Control Architecture: Unlike previous studies, this work introduces an innovative Model Predictive Control (MPC) based hierarchical control that is designed specifically for hybrid shipboard microgrids. While conventional control methods like PI and SMC have been explored in Ni et al. (2021) Mosayebi et al. (2020), Ansari et al. (2020), we propose an optimized MPC framework that leverages dynamic system modeling to provide more precise control over fluctuating load conditions.
2. It helps to minimize transient spikes of DC link voltage, particularly under variation of load as well as AC/DC grid transition conditions (Mariscotti, 2021; Marimuthu et al., 2023).
3. Involving RESS and DGs: In this research, more than one distribution generators (DG) has been used for the shipboard MG as well with multiple renewable energy resources (RES). This research shows an increased flexibility and scalability as SMG system can handle real-time inclusion, allocation and dispatching strategy for different energy carriers while preserving AC/DC grid transitions.
4. Comparative performance: Investigating and analyzing the relative performances presented for three different control schemes that are PI, SMC, and MPC under static conditions as well dynamic loads novelty in this paper with respect to optimizing energy and resilience of hybrid microgrids system. The manuscript now specifically discusses how MPC excels in rapid response, energy conservation and stability during various types of fault conditions compared to alternatives.

The main contribution of this paper is to devise an optimal hierarchical control architecture fully tailored for hybrid AC/DC shipboard microgrids. These architectures have been developed to solve the problems of energy optimization and fluctuation load with multiple distributed generators (DGs) such as RES (Chen et al., 2024). In contrast with prior works that concentrate on conventional control techniques, the proposed architecture introduces an innovative utilization of Model Predictive Control (MPC) to improve transient response and robustness to parametric variations and disturbances (Lu et al., 2024; MacKinnon et al., 2022).

High computational demand of advanced controllers, and the difficulty in maintaining optimal energy distribution (Azeem et al., 2021). Hence, while traditional methods have focused on either AC or DC microgrids, this research proposes a novel hybrid architecture that integrates both AC and DC components in a shipboard microgrid, ensuring energy optimization across both systems. This dual integration is relatively unexplored in current literature, making it a significant contribution (Nejabatkhan and Li, 2014; Majumder et al., 2009).

The proposed method employs a multi-level hierarchical control architecture, which is specifically designed to improve both the stability and efficiency of hybrid microgrids by incorporating secondary and tertiary control layers. To substantiate the novelty of this work, we compare results against previous studies and present a quantitative comparison that demonstrates that the proposed MPC based control scheme outperforms existing methods for the hybrid AC/DC shipboard microgrid system. This also includes improved voltage stability, enhanced fault tolerance, faster transient response, reduced energy losses, or lower computational costs (Tian et al., 2024).

The claim is further supported by mathematical derivations and the unique scenarios simulated, such as hybrid AC/DC interactions, the integration of multiple RESs, and variable load conditions, which are less explored in the literature. The ability of proposed method to maintain stability and performance under these complex conditions is clear advancement.

- Given the increasing importance of renewable energy in power systems, this work's emphasis on RES integration in microgrids is highly relevant to the current shift toward greener energy solutions for the hybrid SMG.
- The novel use of MPC for real-time optimization aligns with trends in smart grids and automated control systems, areas of active research and industry focus.

This paper responds to the problem of efficiently coordinating energy and power in interconnected AC/DC SMGs, which allow for the operation of multiple RESs and DGs in a shipboard microgrid environment. Such systems involve complicated and dynamic conditions that make conventional control techniques ineffective and produce low efficiency, instability, and power quality problems. The proposed solution includes a new MPC-based hierarchical control structure developed exclusively for shipboard microgrids. By increasing system stability and efficiency in fluctuating loads and hybrid AC/DC grid transition conditions, this architecture represents a step forward for renewable energy in marine applications.

The benefits of a hierarchical control strategy using the MPC approach are outlined below.

1. Enhanced Stability: The method tracks load fluctuations and change-overs between AC and DC grids, reducing transient pulsating in the DC-link voltage and stabilizing the system.
2. Improved Energy Optimization: The structure of the MPC framework eliminates energy losses in power flow in the microgrid system.
3. Fault Tolerance: The hierarchical design improves the system's robustness to parametric perturbations and random interferences, thus guaranteeing optimal performance under unfavorable conditions.
4. Scalability and Flexibility: The operation of the various RESs and DGs is coordinated to form a scalable structure whereby the system can balance and distribute energies from different sources and customers.
5. Superior Performance: Unlike conventional controller techniques, the MPC approach delivers an optimal response during transients, superior fault and disturbance recoveries, and finer control during dynamic operating modes and environments.
6. Real-Time Optimization: MPC's predictive characteristic makes it easy to manage non-linear, dynamic conditions and guarantees that the exerted control actions are the best possible ones in all conditions.

These advantages make the proposed method a robust and reliable solution for managing the complex dynamics of hybrid shipboard microgrids.

In the control design section, we separate the description of the hierarchical control framework and the individual control strategies

into distinct subsections. This allows us to methodically explain the MPC design, including the formulation of the cost function, constraints, and tuning methodology, without overwhelming the reader with too much information at once (Xie et al., 2021a; Ma et al., 2020; Ding and Yang, 2024). Grouping the cost function and constraints together in a summarized format further streamlines the presentation of the MPC problem statement (Elnawawi et al., 2022). The discussion includes a thorough explanation of how the tuning of the Q and R matrices influences the MPC's performance, and we provide a sensitivity analysis to demonstrate the impact of different design parameters.

The structure of this paper includes Section 2 encompasses the details of the modeling and design of a hybrid AC/DC SMG. Section 3 discusses the primary control structure. Section 4 discussed the secondary control structure of SMG in which we proposed the MPC based design for the system. Section 5 discussed the tertiary control structure. Simulation findings are discussed in Section 6. Hardware implementation details and results are presented in Section 7, and conclusions and future directions have been presented in Section 8.

2. Modeling and design of hybrid AC/DC SMG

Fig. 1 shows how distributed RES and BESS microgrids with converter-interfaced microgrids are organized. According to the illustration in the figure, a microgrid can be connected to various kinds of microgrids by using a range of converters. Model predictive-based cost function and solution procedure are essential components of MPC's control structure (Zhang et al., 2022; Lu et al., 2024). In contrast, the standard design process typically follows three stages:

1. Establishing the predictive model
2. Designing the cost function
3. Configuring the solution algorithm

The MPC is a control strategy that maximizes the value of a system model within certain constraints in order to maximize control signals or instructions by minimizing a set of specified cost functions (Nguyen and Jung, 2018). Microgrids' converter-level and grid-level MPC may appear to be distinct from one another. Switching signals are produced by the former drive power converters, and the latter dispatches DGs and controlled loads in accordance with its instructions. However, the MPC architecture shared by both of these tiers allows for a consistent control structure and design process.

2.1. MPC at the converter level

Two types of MPC strategies have been used with converters. First is Finite control set model predictive control (FCS-MPC), and second is continuous control set model predictive control (CCS-MPC) (Zhang et al., 2022). Nevertheless, FCS-MPC involves discrete actions of converters and does not need Pulse Width Modulation (PWM) regulators to drive converters, CCS-MPC produces periodic signals to generate the PWM controller to drive converters. Over the past few years, FCS-MPC has been widely used in a number of industries (Mutarraf et al., 2019).

Consequently, FCS-MPC represents a significant subset of MPCs. **Fig. 2** depicts the comprehensive idea of converter-level MPC with the one-horizon prediction. The acquisition of state variables, such as voltage, current, and power, by measurement or estimate yields the predictive model of RLC circuit dynamics. The switching state represents the gating signal frequency for the inverter, which generates the pulsating AC output voltage, which is further passed through filter by the RLC circuit to produce a pure sinusoidal voltage signal for load utilities. The switching state represents the gating signal frequency for the inverter, which generates the pulsating AC output voltage, which is further passed through filter by the RLC circuit to produce a pure sinusoidal voltage signal for load utilities. State variables $\tilde{x}(k+1)$ at

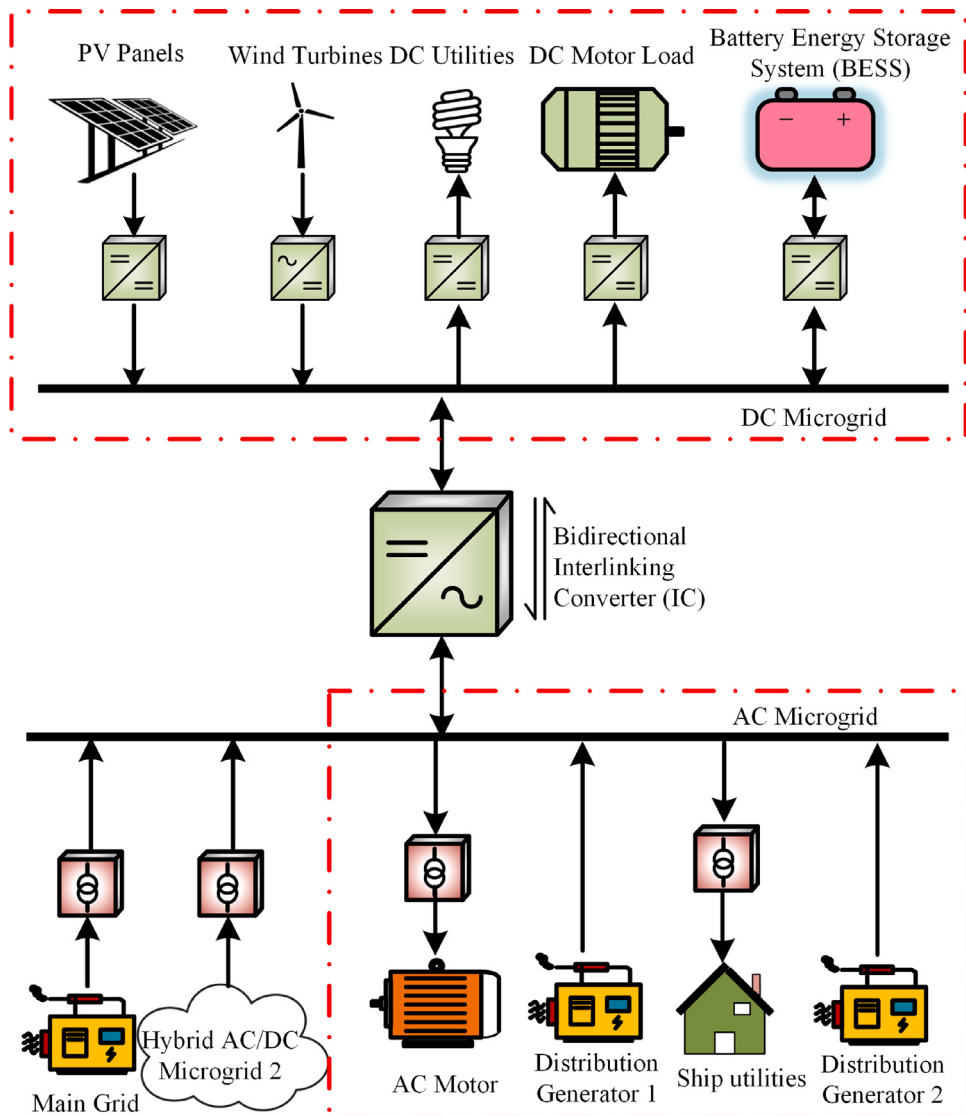


Fig. 1. Single line diagram of hybrid SMGs.

the next instance $k + 1$ can be predicted. The generalized cost function for this configuration can be represented as

$$\tilde{x}(k+1) = f(x(k), u(i)) \quad (1)$$

Here $x(k)$ represents the state of the RLC circuit at instance k , $u(i)$ is one of a limited number of possible switching states for the converter, and function $f(\cdot)$ satisfies Kirchhoff's Voltage Law (KVL) equations. The typical form of the cost function can be represented as

$$h = \sum (w_o |u^* - \tilde{x}(k+1)|) \quad (2)$$

Here \tilde{x} represents the state of the RLC circuit at a future instant $(k + 1)$, u^* is the switching frequency reference input signal for the converter, and w_o is the optimal weighting coefficient. In most cases, algorithms that do exhaustive searches are effective (Clarke et al., 2016). However, grid-level MPC uses a specialized toolbox to simplify a more involved method (Hou et al., 2020). It is important to observe that Fig. 2 may be used with a wide range of converter typologies (Mutarraf et al., 2022).

The goal of the MPC is to optimize the control inputs over a prediction horizon to minimize a cost function, subject to system dynamics and constraints (Alsmeier et al., 2024). The problem can be formulated for the MPC aims to minimize a quadratic cost function over

a prediction horizon N can be given as (Chen et al., 2024)

$$J = \sum_{k=0}^{N-1} (x_k^T Q x_k + h_k^T R u_k) + x_N^T Q_f x_N \quad (3)$$

Where J is function that needs to be minimized, x_k and u_k are state and input vectors with index k . Q and R are weight matrices for MPC control input. The cost function balances the tracking error (minimizing the deviation of the states from the desired reference) and the control effort.

The overall MPC optimization problem is subjected to minimizing the quadratic cost function J by optimizing the control inputs u_k . Furthermore, ensure that the system dynamics are respected using the state-space equations and impose limits on the state and control input values to ensure safe and feasible operation.

In future research, the goal be to implement this hierarchical control design in real-time. We approach this by addressing the computational cost of solving the optimization problem at each level of the controller, with a focus on ensuring that the controller can operate within the time constraints imposed by the microgrid's dynamics.

We explore the use of real-time optimization algorithms such as dual-decomposition methods or fast gradient methods that reduce the computational burden of solving the MPC problem at each time step (Lu et al., 2024). Moreover, we plan to implement the MPC controller on

embedded platforms such as FPGAs or DSPs (Digital Signal Processors) that are capable of performing high-speed computations while meeting the real-time demands of the system. To lower computational complexity, we experiment with adaptive prediction horizons, where the controller adjusts the length of the horizon based on the system's dynamic conditions (MacKinnon et al., 2022). This allows for shorter, faster calculations during stable periods and more detailed calculations during rapid changes. Before deployment, we validate the real-time performance of the MPC controller using Hardware-in-the-Loop (HIL) simulations, which replicate the physical system's behavior in a controlled environment. This step is crucial to assess and refine the computational efficiency of the controller under real-world timing constraints (Yfantis, 2024).

To further enhance clarity, we include equations that define the cost function J in terms of the quadratic penalties on the output deviations and control inputs, along with the associated matrices Q and R . The cost function expressed as a summation over the prediction horizon, accounting for both the state regulation and control effort (Bledt, 2020). We also provide explicit equations for the constraints imposed on the system, such as input limitations, voltage, and current bounds, as well as any operational constraints related to the bidirectional converters in the AC/DC microgrid. These constraints are integrated into the overall MPC optimization framework, and their impact on control performance is discussed in the context of ensuring system stability and operational safety under varying conditions (Jain, 2020).

Significant advancements have been made in converter-level MPC over the past few years. Generalized predictive control (GPC) and explicit MPC are its most popular offshoots because CCS-MPC generates a consistent switching frequency, GPC and an LCL filter were used to address harmonics (Roy et al., 2023). The input-output model was built using a neural network core and an explicit MPC for DC-DC converters in research (Chen et al., 2020). Research that takes into consideration the control time sequence is one of the most promising new avenues in FCS-MPC, by using a deadbeat strategy to control in order to manage the time sequence effectively (Hou et al., 2019). Enhancements to the FCS-MPC resulted in the concurrent achievement of a consistent switching frequency and enhanced steady-state performance (Wang et al., 2020a).

In the last decade, notable advancements have occurred in MPC at the converter level. Since CCS-MPC generates a constant switching frequency, GPC and explicit MPC are its most common offshoots. To address harmonics, GPC was combined with an LCL filter in Judewicz et al. (2018), Lima et al. (2017). MPC specifically for DC-DC converters was integrated with a neural network architecture for constructing the input-output model. One of the most promising new directions in FCS-MPC is research that takes into account the control time sequence. On the other hand, a deadbeat approach to improve the control timing sequence for current regulation within a single control period. Moreover, they enhanced FCS-MPC, achieving both stable switching frequency and improved steady-state performance simultaneously.

2.2. DC microgrid modeling

Fig. 3 shows the schematic diagram of a VSC we used for modeling the Interlinking Converter (IC). Here, KVL can be applied to the equation of the DC microgrid system, specifically at the DC source end. When a DC source is connected to a battery that maintains a constant voltage, it is essentially linked to this battery (Lee et al., 2021). Furthermore, the DC load in this scenario is characterized as a constant power load. According to KVL within the DC microgrid, the DC source voltage is determined by summing the load voltage and the voltage difference across line losses (Alam et al., 2016).

$$V_{dc,s} = i_{dc,line} R_{dc,line} + V_{dc,load} \quad (4)$$

In the case of a constant power load, the value of $P_{dc,load}$ remains constant and can be represented as

$$V_{dc,s} = i_{dc,line} R_{dc,line} + \frac{P_{dc,load}}{i_{dc,load}} \quad (5)$$

2.3. AC microgrid modeling

Applying KVL at AC load side

$$v_{inv} = E_{inv} + Ri_{inv} + L \frac{d}{dt} i_{inv} \quad (6)$$

Where E_{inv} is the three phase terminal voltage of inverter, v_{inv} is the inverter voltages. Above equation can be written as

$$\frac{d}{dt} i_{inv} = \frac{v_{inv}}{L_{inv}} - \frac{R_{inv}}{L_{inv}} i_{inv} - \frac{E_{inv}}{L_{inv}} \quad (7)$$

Utilizing the dq -transformation on three-phase currents

$$\frac{d}{dt} i_{inv}^d = \frac{v_{inv}^d}{L_{inv}} - \frac{E_{inv}^d}{L_{inv}} + \omega i_{inv}^q - \frac{R_{inv}}{L_{inv}} i_{inv}^d \quad (8)$$

and

$$\frac{d}{dt} i_{inv}^q = \frac{v_{inv}^q}{L_{inv}} - \frac{E_{inv}^q}{L_{inv}} - \omega i_{inv}^d - \frac{R_{inv}}{L_{inv}} i_{inv}^q \quad (9)$$

The state space model of (8) and (9) can be represent as

$$\begin{bmatrix} \dot{x}_1 \\ \dot{x}_2 \end{bmatrix} = \begin{bmatrix} -\frac{R_{inv}}{L_{inv}} & \omega \\ -\omega & -\frac{R_{inv}}{L_{inv}} \end{bmatrix} \cdot \begin{bmatrix} x_1 \\ x_2 \end{bmatrix} + \frac{1}{L_{inv}} \begin{bmatrix} u_1 \\ u_2 \end{bmatrix} - \frac{1}{L_{inv}} \begin{bmatrix} E_{inv}^d \\ E_{inv}^q \end{bmatrix} \quad (10)$$

The leading principal minor of matrix A has a negative definite value, indicating that the system will exhibit asymptotic stability over an indefinite duration.

2.4. MPC at the grid level

Unlike converter-level MPC, Grid-level MPC seeks to regulate macro-level operational states such as microgrid power flows or BESS capacity. To maximize the effectiveness of limited systems seeking to satisfy numerous goals, grid-level MPC can be used as an optimization technique. Using the present and historical states of the system, a predictive model is constructed that can provide predictions about the future state of the system (Mutarraf et al., 2019). Specific examples of time-interval-based state variables that may be predicted by a predictive model include load needs, electricity costs, PV, and wind turbines (WT) as shown in **Fig. 1**.

The control goals should inform the development of the cost function. Items in a cost function usually correspond to the various goals of control or optimization. This cost function is a formulation of the predictions from the predictive model and potential goals. Over the course of each sample interval, the optimal control/command sequence for the entire system is calculated. After that, the cost function is modified based on a new set of system states, and the process repeats until the horizon has advanced by a one-time step. With a feedback mechanism that successfully lessens the implications of uncertainty, grid-level MPC can offer a shrinking prediction horizon and increased resilience to disruptions.

MPC controllers are utilized to replace cascaded voltage and current loops in the majority of current research on the MPC employed in primary control. For islanded microgrids, ensuring a steady voltage supply is essential, requiring inclusion of voltage formulation within the cost function, various MPC methods are employed. As an illustration, **Fig. 4** presents the schematic representation of the MPC system utilized in the primary control of an islanded AC microgrid together with a representation of the CLC technique. As shown, both MPC-CLC controllers and power calculation use measurements or estimates from the circuit, and these controllers then need the virtual impedance produced by the estimated power droop control. The main benefit of MPC in a microgrid is the quick transient response to manage the varying power outputs derived from renewable energy sources. The design is further simplified by eliminating the PWM modulator.

MPC excels in its capability to predict future system performance as it solves an optimization problem for a finite span of prediction horizon. With the help of MPC, we can plan ahead and anticipate control inputs before time to counteract disturbances or sudden changes in load.

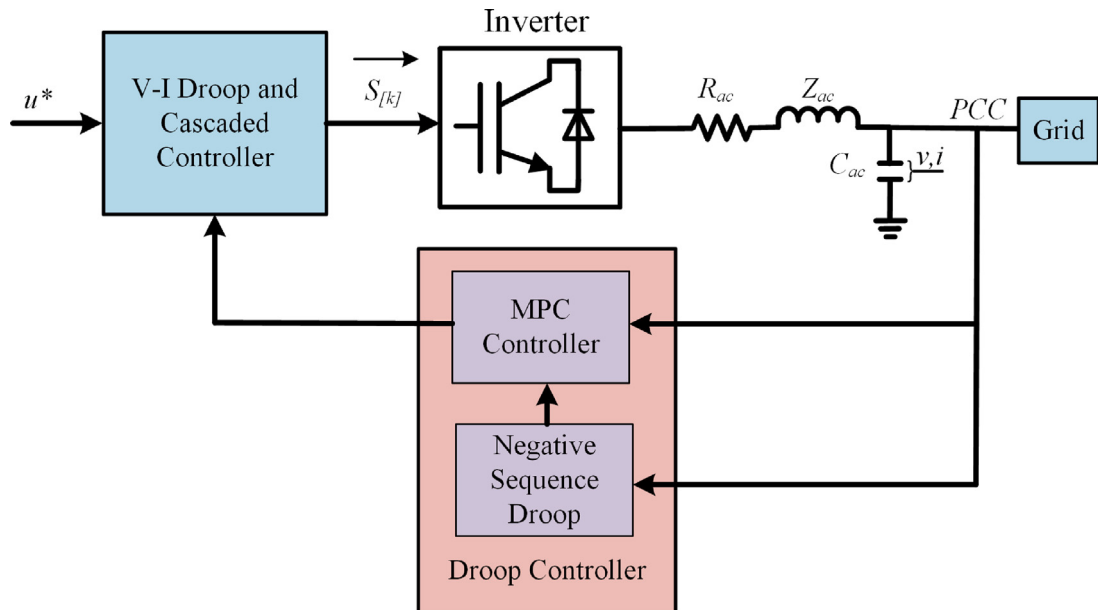


Fig. 2. Converter level MPC model.

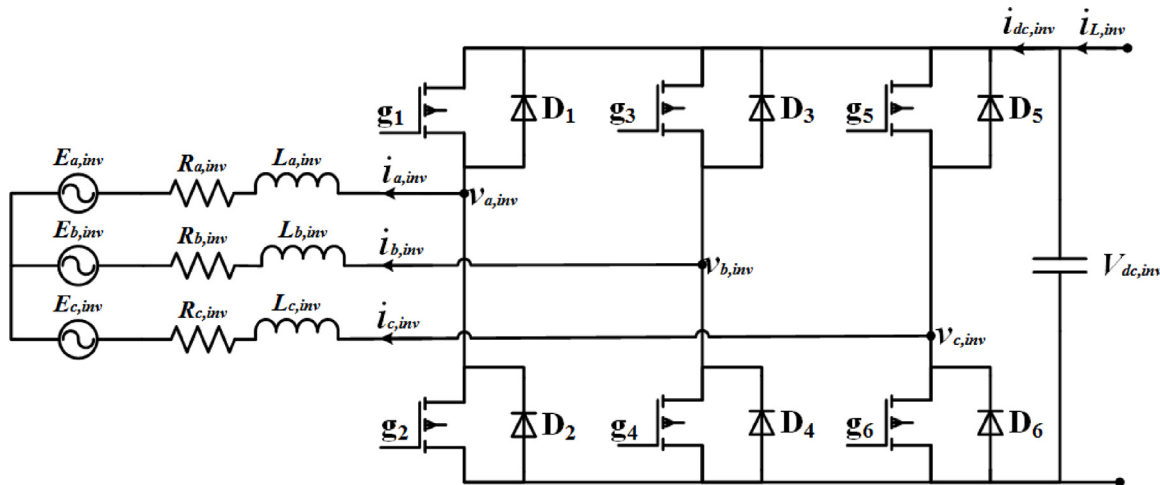


Fig. 3. 2-level voltage source converter (VSC) schematic.

It is because the MPC runs based on a predictive model of the system to define the future states and possible disturbances throughout a defined predication horizon. As such, the MPC is capable of knowing the future state and any possible disturbance insight, which makes it decide on which control actions to adopt before the disturbances take an actuation form, resulting in a quicker response to sudden changes. In contrast, the traditional approaches opt for disturbances after they have occurred, leading to adjustments of control input to alter the effect of anticipated deviations in power output and scenarios of the load variation.

The capability of predicting future states works perfectly in an environmental setting prone to change rapidly and more stable and efficient power demand and generation. Moreover, MPC solves an optimization problem at every control interval maintaining a moving prediction of the future states and system limits. In that case, it decides which is not only an optimal control action but also realistic to avoid system limitations and distortions from the desired set points.

On a real-time basis, the MPC keeps on updating the control strategy to adopt the updated data and predictions to respond to sudden changes such as renewables to sell while others are bumpy or when the load

variations occur suddenly. It is an important factor that helps the system handle transients effectively. Simulation results in the revision work that MPC function is perfect in terms of transient response than traditional such as PI and SMC. It could minimize variations quickly and rectify the system once the deviation occurs.

System stability and performance from microgrids in which power outputs fluctuate quickly due to distributed generators and renewable energy sources. MPCs have the advantage of being able to deal with a many-variable control problem constrained, while this capability is even more useful in these fast-establishing environments. MPC minimizes the deviation from the desired operating point more effectively than traditional controllers, such as PI or PID, which generally react to errors after they happen by constantly updating control actions according to real-time measurements and predictions.

In addition, MPC can take system models and constraints into control design, allowing it to do multiobjective optimization for minimizing energy losses, reducing equipment degradation as well as maintaining power quality. This optimization power, coupled with its ability to respond quickly and effectively to transient states of the grid, makes MPC especially ideal for controlling the broad system changeable microgrid operation.

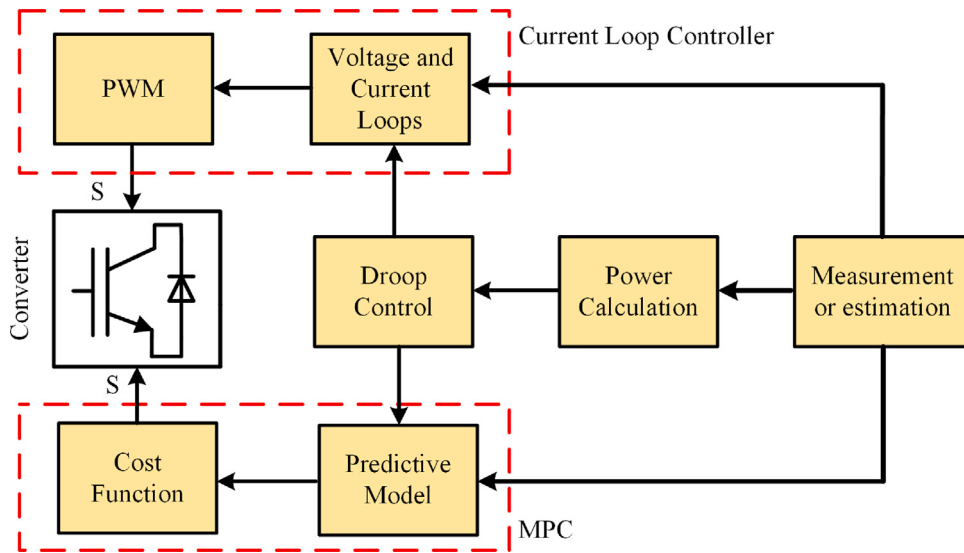


Fig. 4. Grid-level MPC model.

All of the DGs, power converters, power elements, power cables, and utility network grids in question need to be evaluated in light of the constraints. Once the limitations are properly established, the system's performance can be enhanced by allowing it to function inside or very close to the restrictions without compromising safety. After solving the constraint-based optimization issues, the time horizon window will be advanced so that the optimization problems may be computed and solved whenever updated forecasts are available (Fang et al., 2019).

Grid-level MPC often has a longer sampling interval t than converter-level MPC, which can be anywhere from a few seconds to a few hours. Multiple elements often combine to establish the time frame. If, for instance, the PV power production is recorded every minute and the PV generation is projected every 30 min, the prediction will be off by 30 min. For optimal matching and accuracy, the MPC's ultimate sampling interval is predicted to be a multiple of 30 min. The utilization of MPC on the grid level may be summed up as follows.

1. Initially, a receding model is constructed using system states.
2. Based on the data, determine the appropriate control/command sequence for the subsequent prediction period for a given control horizon.
3. Carry out the MPC's initial step while taking into account all relevant factors.
4. Optimize the system once again, going forward one period and updating all available states.

3. Primary control structure of SMG

3.1. Droop control strategies

The most common strategy for voltage and frequency variations is a mathematical representation of the droop equations for the AC side microgrid.

$$f = f^* - \alpha P \quad (11)$$

$$v = v^* - \beta Q \quad (12)$$

Where α and β represent the frequency and voltage droop coefficients, P represents the nominal active power, and Q represents the reactive powers. Whereas f^* and v^* represent the nominal AC frequency and voltage. Similarly, the DC side equation of the microgrid can be given as

$$V_{dc} = V_{dc}^* - I_{dc} R_{dc} \quad (13)$$

Where V_{dc}^* represents the DC voltage reference, I_{dc} is the DC current at the converter's output, and R_{dc} is the resistance used to compensate for the actual DC line resistances. Since DC microgrids do not have reactive power and frequency, the DC voltage reference may drop linearly with rising output current using this droop control formulation.

3.2. Prediction model with extended time horizons

The Euler forward approximation-based converter-level MPC has a short one-step prediction horizon. The following procedures are often used for forecasting further into the future.

1. We assume that all predictive models may be represented in canonical form as

$$x(k+1) = Ax(k) + Bu(k) \quad (14)$$

where A and B are coefficients at the $k+1$ instant.

2. If we take into account one more stage of prediction, we get

$$x(k+2) = Ax(k+1) + Bu(k+1) \quad (15)$$

It is noteworthy to mention that the (15) is also a useful tool for adjusting for the one-step interval inherent in a fully digital controller.

3. A linear extrapolation approach can be used to go to a further prediction horizon N . This method allows for a more detailed study into the future, which has benefits, including system stability and lower switching frequencies Cortes et al. (2012).

To validate the LTI assumption, few first simplify the hybrid SMG design and analysis of proposed control schemes by allowing techniques from linearized theory to be applied. This is a common assumption used to simplify the type of control law developed, as well as for its ideal performance analysis. Nevertheless, we realize that real microgrids aboard ships are nonlinear and time-varying as a result of non-constant load conditions. For example, when antennas or weapons systems come online, the presence of power electronic elements with characteristics varying by operating point and renewables may have a significant role in system operation.

We use system identification techniques to quantify the linearity of the shipboard microgrid under different operating conditions. Here, the linearity of a system is verified by comparing the response of the real system to that of the LTI model to determine if the linear assumption still holds. The frequency response analysis of the LTI system and

dynamic modeling is used to measure the linearity and time-invariance properties of the system.

On the other hand, this method examines the nonlinear and time-varying implications of different system elements. Furthermore, the behavior of power electronics, load dynamics, and renewable sources determine the extent of linearity. Moreover, the effects of these elements on the linear-regressed control strategies are also determined.

Linear interpolation is faster than some nonlinear forecasting methods. Given that MPC requires real-time optimization, it is important to maintain computational efficiency. The use of simple and calculable predictions is necessary, as this should be the fastest component in real-time control strategy: linear extrapolation. The use of linear extrapolation guarantees an efficient implementation, given that MPC will not be computationally expensive.

3.3. Optimization of cost function

The control law optimization is reflected by the cost function, which also serves as a criterion for choosing the best control strategy. When more than one objective is being pursued, a cost function with more than one term is appropriate. Therefore, attention must be paid while designing the weighting function of each term. The efficiency of the system may be altered by adjusting the coefficient ratios. Coefficients are often normalized by dividing by their references in order to get a common value across all units and the weight of the cost function. On the other hand, if one phrase requires special attention, its coefficient will be increased to reflect this importance. This form of compensation, together with the modification of the coefficients, ends up being a trial-and-error procedure that is highly dependent on the in-depth as well as understanding of the control target.

Intelligent algorithms are one useful tool for optimizing the weighting factors. It may improve the system's performance, for instance, by using fuzzy logic control to make decisions about the weighting coefficients to use (Zhaoxia et al., 2019). The reference values for the controls in cost functions are often held constant or made to be ideal. However, there are frequent occasions when estimates of previous state variables that seldom change are selected as the Khooban et al. (2017), Eghedarpour and Farjah (2014), Nguyen et al. (2018).

4. Secondary control structure for SMG

Droop control is widely employed as a powerful way of main control power-sharing at the moment. However, it inevitably causes $\omega-P$ or $\omega-Q$ variations in a steady state because of its intrinsic control constraints. To address this issue and provide a stable connection to the utility grid, secondary control was designed to dampen voltage fluctuations. Here, we go into the research and theory of MPC-based secondary control. In this research, we propose an SMC based secondary controller design for the hybrid SMG (Alam et al., 2022).

4.1. Secondary control design

Considering the droop control characteristic curve to a different configuration setting, which is the essence of secondary control, and giving extra compensation is the core premise of secondary control. Now, (11) and (12) can be expressed as

$$f = f^* \alpha P + \Delta f \quad (16)$$

$$v = v^* \beta Q + \Delta E \quad (17)$$

The two primary types of secondary control are centralized and dispersed. The PI controller techniques provide the backbone of centralized secondary control, but their use necessitates the use of centralized. The use of intricate communication networks for monitoring the point of common coupling (PCC) voltage and frequency poses the risk of a

single point of failure, potentially reducing the overall system reliability. Furthermore, there is a concern that the system's stability could be compromised if the compensation signals transmitted to the primary control deviate from their required values due to a communication delay or a loss of data. In contrast, secondary control that is distributed gained much attention because of the confidence it inspires in its consistency and robustness.

To implement the distributed secondary control, local and nearby information is necessary, which may be provided via a sparse communication network with numerous agents. Data from buses in the DG and nearby DGs will be compared to that from a centralized system. Additionally, the effortless plug-and-play functionality is enabled by distributed secondary hierarchical control (Bernardino and Skogestad, 2024).

A comprehensive mathematical model of every component involved, whether a shipboard microgrid is required in order to perform MPC based hierarchical control at the grid level. In order to build the prediction model while taking into account a variety of uncertainties and limitations, this is the initial phase. A future-value receding equation is then developed using a time series-based technique to show the expected states based on the current states in order to optimize power flow, reduce operating costs, and maximize DG output efficiency, key variables (Babayomi et al., 2020).

Power flow management and optimization pertain to the considerations regarding how the load demands should be allocated among different power sources and energy storage systems. This is done while concurrently addressing the minimization of power losses, maximization of power generation, and optimization of power storage. A particular solver toolbox is typically used to solve the algorithm, acting as a secondary control to the algorithm (Liu et al., 2015).

Data communication networks of varying bandwidths, capacities, and speeds are used to generate and transmit the frequency/voltage compensation signals. As a consequence, the network is vulnerable to delays, which compromises data security, signal freshness, and control efficiency. Hence, the system's resistance and resilience to communication delays need to be thought of as a design requirement. Moreover, shipboard microgrid efficiency might be at risk with secondary control without primary control (Aghdam et al., 2020).

4.2. MPC-based secondary control design

The objective of employing MPC in secondary control is to generate crucial compensation signals denoted as f and v for the primary droop-based control. The MPC based control design architecture is shown in Fig. 5. Within the framework of grid-level MPC architecture, the following three critical aspects need to be addressed.

1. The cost function should include components related to frequency and voltage.
2. Future states and past or current states are typically derived from local and neighboring systems.
3. Employing dedicated toolboxes to streamline programming and problem-solving processes.

In order to get the system's frequency back to normal, an MPC technique was applied. It is shown that the frequency may be brought to nominal levels with greater speed and fewer oscillations than using the traditional PI approach or an upgraded PI controller with a Smith Predictor (SP). A secondary control for adjusting the f and v using a distributed MPC (Lou et al., 2017). Predictive models need local and nearby data, and the YALMIP toolkit is used as a solver. It is discovered that the MPC at the grid level is resistant to a wide range of perturbations. Similar distributed MPC implementations for secondary voltage control are described in Zhuoyu et al. (2017).

MPC is used to describe a strategy for managing frequency across various shipboard microgrids (Liu et al., 2019). It proves that MPC is superior to the conventional PI controller in coping with noise and

lag in data transmission. MPC is utilized to control the frequency and controlling voltage-sensitive loads while taking bus voltage restrictions into account. Now, converting the VSC system given in (10) into the generalized canonical form with initial conditions $x_0 = x(t_0)$.

$$\dot{x}(t) = Ax(t) + Bu(t) \quad (18)$$

$$y(t) = Cx(t) \quad (19)$$

The solution to the state equation is as follows

$$x(t) = e^{A(t-T_0)}x(t_0) + \int_{t_0}^t e^{A(t-\tau)}Bu(\tau)d\tau \quad (20)$$

Consider $t_0 = kh$ and $t = (k+1)h$, then (21) can be given as

$$x(k+1) = e^{Ah}x(k) + \int_{kh}^{(k+1)h} e^{A(kh+h-\tau)}Bu(k)d\tau \quad (21)$$

control input $u(k)$ remains constant during the interval of k and $k+1$. This assumption is typical in discrete-time control systems, where the control signal is updated at discrete intervals and held constant between updates. For simplicity, taking $\psi = kh + h - \tau$, So (22) can be given as

$$x(k+1) = e^{Ah}x(k) + \int_0^h e^{A\psi}Bd\psi u(k) \quad (22)$$

or

$$x(k+1) = Ax(k) + \Pi u(k) \quad (23)$$

Where $\Lambda = e^{Ah}$ and $\Pi = \int_0^h e^{A\psi}Bd\psi$.

On the other hand, the discrete output can be given as

$$y(k) = Cx(k) \quad (24)$$

4.3. Model predictive control design

Now from (23) and (24), we have

$$x(k+1) = Ax(k) + \Pi u(k) \quad (25)$$

$$y(k) = Cx(k) \quad (26)$$

where $\Lambda \in R^{n \times n}$, $\Pi \in R^{n \times m}$ and $C \in R^{n \times n}$. Using the differential method as

$$\Delta x(k+1) = x(k+1) - x(k) \quad (27)$$

The state Eq. (25) become

$$\Delta x(k+1) = \Lambda \Delta x(k) + \Pi \Delta u(k) \quad (28)$$

where $\Delta u(k+1)$ can be expanded as $u(k+1) - u(k)$. Similarly, by applying the backward difference at the output Eq. (26), we get

$$\Delta y(k+1) = y(k+1) - y(k) \quad (29)$$

By expanding $y(k+1)$ and $y(k)$, we get

$$\Delta y(k+1) = Cx(k+1) - Cx(k) \quad (30)$$

Using (27), we get

$$\Delta y(k+1) = C \Delta x(k+1) \quad (31)$$

If C is Invertible: If the matrix C is known to be invertible, the correct transformation would be:

$$\Delta x(k+1) = C^{-1} \Delta y(k+1) \quad (32)$$

If C is not invertible, the transformation cannot be done directly by simple inversion. Use the Moore–Penrose pseudo-inverse C^+ if C is not square or is singular.

$$\Delta x(k+1) = C^+ \Delta y(k+1) \quad (33)$$

Now substituting in (28), we get

$$\Delta y(k+1) = C \Lambda \Delta x(k) + C \Pi \Delta u(k) \quad (34)$$

or we can write it as

$$y(k+1) - y(k) = C \Lambda \Delta x(k) + C \Pi \Delta u(k) \quad (35)$$

which leads to

$$y(k+1) = y(k) + C \Lambda \Delta x(k) + C \Pi \Delta u(k) \quad (36)$$

Combining (28) and (36), we get

$$\begin{bmatrix} \Delta x(k+1) \\ y(k+1) \end{bmatrix} = \begin{bmatrix} \Lambda & O \\ C \Lambda & I_P \end{bmatrix} \cdot \begin{bmatrix} \Delta x(k) \\ y(k) \end{bmatrix} + \begin{bmatrix} \Pi \\ C \Pi \end{bmatrix} \Delta u(k) \quad (37)$$

and output Eq. (26) can be given as

$$y(k) = [O \quad I] \cdot \begin{bmatrix} \Delta x(k) \\ y(k) \end{bmatrix} \quad (38)$$

Defining

$$\hat{x}(k) = \begin{bmatrix} \Delta x(k) \\ y(k) \end{bmatrix} \quad (39)$$

Let change of variables can be shown as

$$\hat{\Lambda} = \begin{bmatrix} \Lambda & O \\ C \Lambda & I_P \end{bmatrix}, \quad \hat{\Pi} = \begin{bmatrix} \Pi \\ C \Pi \end{bmatrix}, \quad \hat{C} = [O \quad I] \quad (40)$$

Using (37) and (38),

$$\hat{x}(k+1) = \hat{\Lambda} \hat{x}(k) + \hat{\Pi} \Delta u(k) \quad (41)$$

$$y(k) = \hat{C} \hat{x}(k) \quad (42)$$

The minimum cost function can be derived by

$$J(\Delta U_N) = \frac{1}{2} (r_p - Y)^T Q (r_p - Y) + \frac{1}{2} \Delta U_N^T R \Delta U_N \quad (43)$$

where $Q = Q^T > 0$ and $R = R^T > 0$. We have real symmetric Q and R positive definite. The introduction of the scalar $\frac{1}{2}$ serves the purpose of simplifying subsequent calculations. Moreover, the vector r_p comprises command signal values recorded at specific sampling intervals. The choice of weight coefficients Q and R is driven by an unique control law $J(\Delta U)$, which aims to maintain a small tracking error $|r_p - Y|$ while ensuring that control actions remain minimum.

Y represents the output matrix, which includes the system's measurable states or outputs that we aim to control or regulate. For example, voltage, power, or current at the load side of the microgrid. U_N represents the input matrix, which consists of the control inputs or manipulated variables used to influence the system's behavior over the prediction horizon.

The prediction horizon N in MPC refers to the number of future time steps over which the controller predicts system behavior and optimizes the control inputs. N further represents the length of the prediction horizon, and it directly impacts the accuracy and performance of the control strategy.

The choice of N affects the balance between computational complexity and control performance. A longer prediction horizon generally leads to better optimization and more accurate future state predictions but at the cost of increased computational effort (Verheijen et al., 2024). Conversely, a shorter horizon reduces computational burden but sacrifices control performance, particularly in systems with long-term dynamics (Esfahani and Velni, 2024).

To address the sensitivity of the results to the horizon length, we plan to conduct future studies to analyze how different horizon lengths influence performance metrics such as response time, stability, and energy optimization in real-time applications (Sarwar et al., 2022).

- Initially, a trial and error approach was used to choose the Q and R matrices by manually adjusting them to balance performance between state regulation and control effort.
- A high value for Q prioritizes minimizing state deviations from the reference trajectory, while a high value for R minimizes the control effort, preventing aggressive control actions.

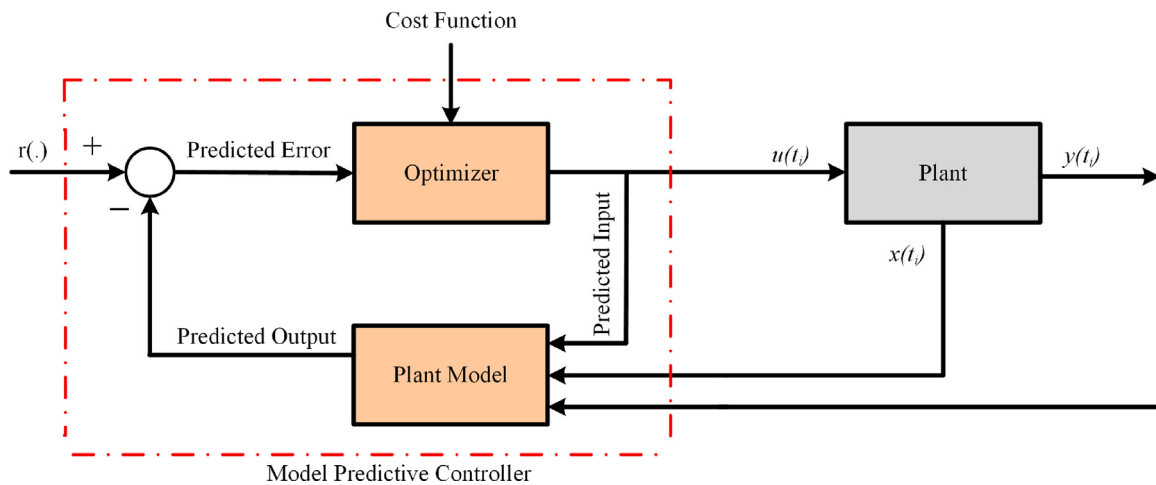


Fig. 5. MPC design block diagram.

These matrices were further fine-tuned using heuristic methods based on system dynamics and preferred criteria, such as the optimum response time and minimum overshoot. However, larger weights were set on several states, such as DC-link voltage stability and power balance between AC and DC parts (Wang et al., 2020b). Unique system characteristics such as converters' power capacity and the system's tolerance to load increase were also considered. In dynamic simulations, the focus was rested on maintaining the deviation between the crucial states during transients. Thus, Q was increased, and R was decreased, respectively (Dahane and Sharma, 2024).

For static load conditions, R was increased to reduce control actions and maintain system stability without critical state pole deviation. In the work with multiple DGs and RESs, Q was set on minimizing the deviation from the power balance, while R was adjusted to smooth transitions from one source to the other to prioritize maintaining the balance between renewable and conventional sources, while the R matrix was adjusted to ensure smooth transitions between different power sources (Zafari et al., 2020).

Under faulty load conditions, the matrices were adjusted to quickly restore stability. This required a higher emphasis on Q to minimize deviations in critical states like DC-link voltage, while R was adjusted to avoid over-stressing the converters during fault recovery (Xie et al., 2021b).

5. Tertiary control of a shipboard microgrid

In order to achieve adaptable interaction between networked SMGs or between the SMG and utility grid, tertiary control plays a significant role. At this supervisory command, the flow of power and the efficiency of economic activities are prioritized. When solving optimization problems that include several constraints, grid-level MPC is often used.

5.1. Principle of tertiary control

Whether within or outside of a MG, all relevant components must be represented mathematically for MPC control to be implemented at the grid level. Furthermore, this is the initial stage in developing a prediction model that takes into account a wide range of conditions.

Consequently, a future-value receding equation is formulated using a time series-based approach. This equation shows the expected states. Predictions will typically include data on DG outputs, power pricing, and load demands critical elements for maximizing DG output efficiency, minimizing running costs, and optimizing power flow (Shagar et al., 2017). Distribution of load requirements among different power sources and BESS is a key aspect of power flow management and

optimization, which must also take into account minimizing power loss, maximizing power output, and optimizing power storage (Jin and Yang, 2023).

Here are some of the benefits that MGs may get by using MPC as a tertiary control.

- Incorporating multiple objectives into the cost function by an easy quadratic summation.
- Giving careful consideration to a wide variety of constraints within reasonable bounds.
- Making use of a specialized toolbox equipped with a potent solver to streamline the algorithm-solving process, all of which are especially useful for tertiary-level control.

5.2. Power optimization and management using MPC

In order to create a workable plan for power transfers inside or across shipboard microgrids, several criteria must be satisfied. Interactions between the microgrid and the power utility often include this kind of economic optimization pertinent to power management. For instance, MPC was used to optimize the flow of power in a microgrid that was linked to the grid (Yamashita et al., 2021).

A shipboard microgrid was modeled in its entirety, including power storage and power needs, in order to construct an MPC predictive model for more efficient power energy dispatch In Nassourou et al. (2017). Microgrid power management is improved with the use of a distributed MPC that takes environmental and monetary considerations into account (Zheng et al., 2018). According to research (Jia et al., 2020), a distributed MPC was developed for the purpose of achieving economic optimization by factoring in the cost/benefit of energy sources, the expenses associated with electricity sales, and the charges related to selling electricity were mentioned. Additionally, there was a fifth phase related to the utilization of battery power (Kou et al., 2017; Huang and Qahouq, 2014).

Similarly, formalized the cost functions associated with either acquiring energy from or selling energy to the microgrid, and they offered a novel distributed economic MPC method to maximize the benefits for microgrid users (Sachs and Sawodny, 2016). Moreover, paper Morstyn et al. (2016) proposes a probabilistic MPC method employed to balance the power within a microgrid while considering available exchange power. This approach can be applied to determine the optimal power references for both Wind Turbines WTs and Electric Vehicles electric vehicles (EVs) (Morstyn et al., 2018).

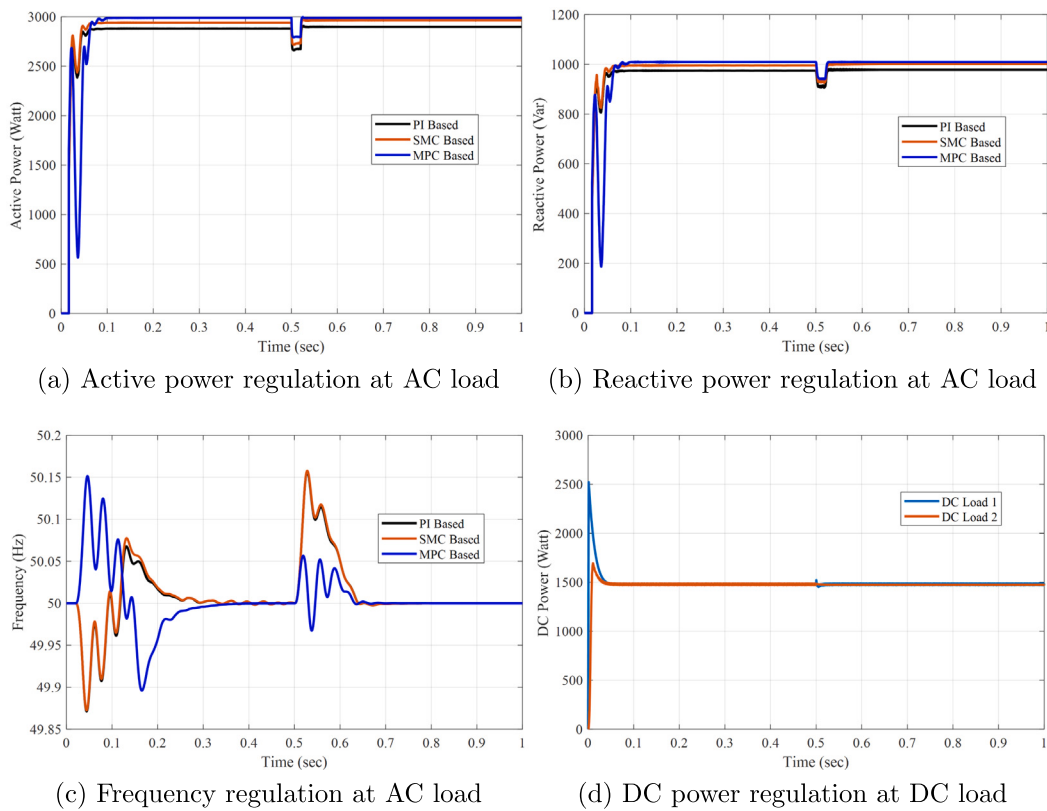


Fig. 6. Case 1 : Power flowing from MG1 to MG2; then MG2 to MG2 side.

5.3. MPC at the grid level for interconnected microgrids

Increasingly, people are worried about networked microgrids, which are groups of microgrids that are electrically linked to one another in order to handle additional RESs and loads. This interconnected design encourages the use of renewable energy sources by allowing tiny AC/DC MGs to provide power assistance for one another. DNO and distribution energy management systems (DEMS) are often required to generate/transmit control instructions and regulate power flows to allow for this interaction. More efficient power optimization is required since the power coordination of interconnected microgrids is more complicated than that of standalone microgrids.

The power distribution in a microgrid was coordinated using a centralized MPC (Yang et al., 2019). Upper and lower bounds are placed on the prediction model. The first portion of the cost function concerns itself with neighboring microgrids and the second with the utility grid, both of which are involved in the exchange of energy. To reduce operational costs and maintain a power balance in the face of uncertainty in both supply and demand, MPC was utilized (Karnavas and Nivolianiti, 2023). Appropriate measures may be taken to accommodate different restrictions using the MPC's dynamic receding-horizon method. To maximize economic value while minimizing deterioration of storage systems exposed to varied limitations by developing a distributed MPC (Garcia-Torres et al., 2019).

6. Simulation results

The simulation tests were conducted to evaluate the performance of an optimized controller proposed for a hybrid shipboard microgrid. In this simulation, we employed two identical models of the hybrid MG1 and MG2. Considering 3 kW active loads, a 1 kVar inductive load is linked in parallel with circuit breakers and lumped impedances in the transmission line. The AC side shipboard microgrid operated at a frequency of 50 Hz and was connected to a distribution transformer and

LCL filter units, enabling it to share power with the DC side shipboard microgrid through an IC. The IC between AC/DC shipboard microgrid is operating as a 2-level VSC, allowing bidirectional power flow based on load requirements.

Conversely, the DC microgrid includes DC sources such as BESS and PV solar panels, alongside DC resistive loads and transmission line resistance. The nominal voltage for the DC microgrid was set at 550 volts, with two 1.5 kW resistive loads connected via circuit breakers.

The core objective of the hierarchical secondary controller is to monitor the line current information for both MG1 and MG2 to generate reference signals for their local primary droop controllers. The implementation and testing of this proposed controller were carried out using MATLAB/Simulink. The simulation parametric values are given in Table 1.

The simulation aimed to compare the performance of conventional PI and SMC based secondary controller with the proposed MPC based secondary control strategies for the hybrid SMGs. Specifically, we focused on the transition from MG1 to MG2, which occurred at simulation time $t = 0.5$ s. Prior to this transition $0 < t < 0.5$ s, both the MG1 and MG2 were powered by the DC source, supplying power to both MG1 and MG2 loads. After $t = 0.5$ s, the DC source of MG2 took over, providing power to both MG1 and MG2 loads from $t = 0.5$ s to $t = 1.0$ s.

6.1. Case 1 : Power flowing from MG1 to MG2 side; then MG2 to MG1 side

Fig. 6(a) illustrates the power variation of AC loads within the hybrid shipboard microgrid. In this plot, the black line represents the AC load power response of PI based secondary controller, the red line signifies the response of the SMC-based controller, and the blue line denotes the response of the MPC-based secondary controller. Initially, MG1 provides power to the interlinking converter, which functions as an inverter, catering to the power demands of both MG1 and MG2. During the time interval $0 < t < 0.5$ s, the performance

Table 1
Shipboard Microgrid parameters for simulation.

Parameters	Description	Rating (Nominal)
f	Frequency	50 Hz
$P_{dc,load}$	DC Load power	1.5 kW
$P_{ac,load}$	Active power of AC load	3 kW
$Q_{ac,load}$	Reactive power of AC source	1 kVAR
$v_{dc,s}$	Voltage of DC source	550 V
$v_{ac,s}$	Voltage of AC source	400 V
L_f	Filter inductance	4 μ H
C_f	Filter capacitance	500 μ F
f_s	Switching frequency	2 kHz
$R_{ac,line}, L_{ac,line}$	line impedance	0.8 Ω , 1.5 μ mH
$R_{dc,line}$	DC line impedance	0.50 Ω

of the proposed MPC-based secondary control surpasses that of the conventional controllers. This is evident as the load power is precisely regulated at 3 kW when using the MPC-based controller. Whereas the SMC and PI controllers maintain load powers at 2.9 kW and 2.8 kW, respectively. Consequently, the discrepancy in load power amounts to $\Delta P_{load}^{PI} = 200$ W and $\Delta P_{load}^{SMC} = 100$ W. Subsequently, between $0.5 < t < 1.0$ s, the microgrid transitions take over the power supply to both MG1 and MG2 loads.

Fig. 6(b) shows the reactive power variations during the microgrid transitions. Here, we can observe that the performance of reactive power by applying MPC based secondary controller is optimal as compared to the other controllers. The reactive power variation can be measured for proposed and conventional controllers are $\Delta P_{load}^{MPC} = 50$ VAR and $\Delta P_{load}^{PI,SMC} \approx 100$ VAR.

Fig. 6(c) depicts the frequency variations on the AC grid. Initially, we can observe that PI and SMC-based controllers initially reduced the frequency because they are dependent on error signals generated from reference and system output. However, our proposed optimal control design has the system's information so that it predicts and produces the control signal, which nullifies the effect system's initial response. In this context, the frequency control achieved by the SMC-based controller results in better frequency regulation and a stable response compared to conventional control methods. While both the PI and SMC-based controllers exhibit frequency variations, the MPC-based controller effectively maintains a smooth regulation at 50 Hz. The frequency droop due to change over is observed $\Delta f_{load}^{MPC} = 0.05$ Hz compared to $\Delta f_{load}^{PI,SMC} = 0.15$ Hz.

Fig. 6(d) shows the DC load power of both MG1 and MG2. We can see that both DC load of MG1 and MG2 are stable and regulated to 1.5 kW. Furthermore, the DC load power is not much influenced by grid transitions or fault conditions.

6.2. Case 2 : Power flowing with AC load increments & MG transitions

Fig. 7(a) shows the comparison of conventional and proposed MPC based secondary controller AC load power variations due to microgrid changeover. Initially, the grid is operating from DC source of MG1. The AC load power is initially regulated to 3 kW. After time $t = 0.5$ s, grid changeover occurs, and we can see a power dip due to voltage drops. The power dip was $\Delta P_{load}^{PI,SMC} \approx 200$ W by using the conventional secondary controller technique. However, it is improved by a 100 W power dip due to grid changeover. Furthermore, the 1 kW step load increments were also observed, and there is a study of state deviations also seen using conventional controllers.

Fig. 7(b) shows the reactive power variations during the microgrid transitions. Here, we can observe that the performance of reactive power by applying MPC based secondary controller is optimal as compared to the other controllers. The reactive power variation can be measured for proposed and conventional controllers are $\Delta P_{load}^{MPC} = 100$ VAR and $\Delta P_{load}^{PI,SMC} \approx 250$ VAR.

Fig. 7(c) compares conventional and proposed secondary controller-based frequency variations due to microgrid changeover as well as

load power increments. The 1 kW step load increases at $t = 0.3$ s and $t = 0.8$ s. Here we can notice a significant improvement in frequency droop response by employing a secondary controller strategy which is $\Delta f_{load}^{MPC} = 0.12$ Hz compared to $\Delta f_{load}^{PI,SMC} = 0.15$ Hz.

Fig. 7(d) shows the DC load power of both MG1 and MG2. We can see that both DC load of MG1 and MG2 are stable and regulated to 1.5 kW. Since MG2 supplies power $t > 0.5$ s, DC load of MG1 power slightly drops due to load increments and grid changeover.

6.3. Case 3 : Power flow from grid connected to islanded mode

Fig. 8(a) illustrates the power variation of AC loads within the hybrid shipboard microgrid. Initially, a main grid is providing power to both the MG1 and MG2. Here, we can see smooth power flow during $0.5 < t < 1.0$ s. Subsequently, the main grid is disconnected at $t = 0.5$ s. Now, the power demand needs to be fulfilled within the shipboard microgrids. Therefore, MG1 starts providing the power to both the MG1 and MG2 without the interception. In this case, we observed the performance of the proposed MPC-based secondary control is significantly better than that of the conventional controllers. At $t > 0.5$ s, the load power is precisely regulated at 3 kW when using the MPC-based controller. Whereas the PI based controller maintains load powers at 2.8 kW. Consequently, the dip in load power amounts to $\Delta P_{load}^{MPC} = 300$ W and $\Delta P_{load}^{PI,SMC} = 2000$ W.

Fig. 8(b) shows the reactive power variations during the microgrid transitions. Here, we can observe that the performance of reactive power by applying MPC based secondary controller is optimal as compared to the other controllers. The reactive power variation can be measured for proposed and conventional controllers are $\Delta P_{load}^{MPC} = 200$ VAR and $\Delta P_{load}^{PI,SMC} \approx 600$ VAR.

Fig. 8(c) depicts the frequency variations on the AC grid. In this context, the frequency control achieved by the SMC-based controller results in better frequency regulation and a stable response compared to conventional control methods. While both the PI and SMC-based controllers exhibit frequency variations, the MPC-based controller effectively maintains a smooth regulation at 50 Hz. The frequency droop due to change over is observed $\Delta f_{load}^{MPC} = 0.195$ Hz compared to $\Delta f_{load}^{PI,SMC} = 0.25$ Hz.

Fig. 8(d) shows the DC load power of both MG1 and MG2. We can see that both DC load of MG1 and MG2 are stable and regulated to 1.5 kW. Furthermore, the DC load power is not much influenced by grid transitions or fault conditions.

6.4. Case 4 : Power flow from grid connected to islanded mode with load variations

Fig. 9(a) illustrates a comparison between the traditional approach and the proposed MPC-based secondary controller in terms of AC load power fluctuations resulting from microgrid transition and load changes. Initially, a main grid is providing power to both the MG1 and MG2. Here, we can see smooth power flow during $0.5 < t < 1.0$ s. Moreover, a 1 kW load increased at $t = 0.3$ s, which can be seen

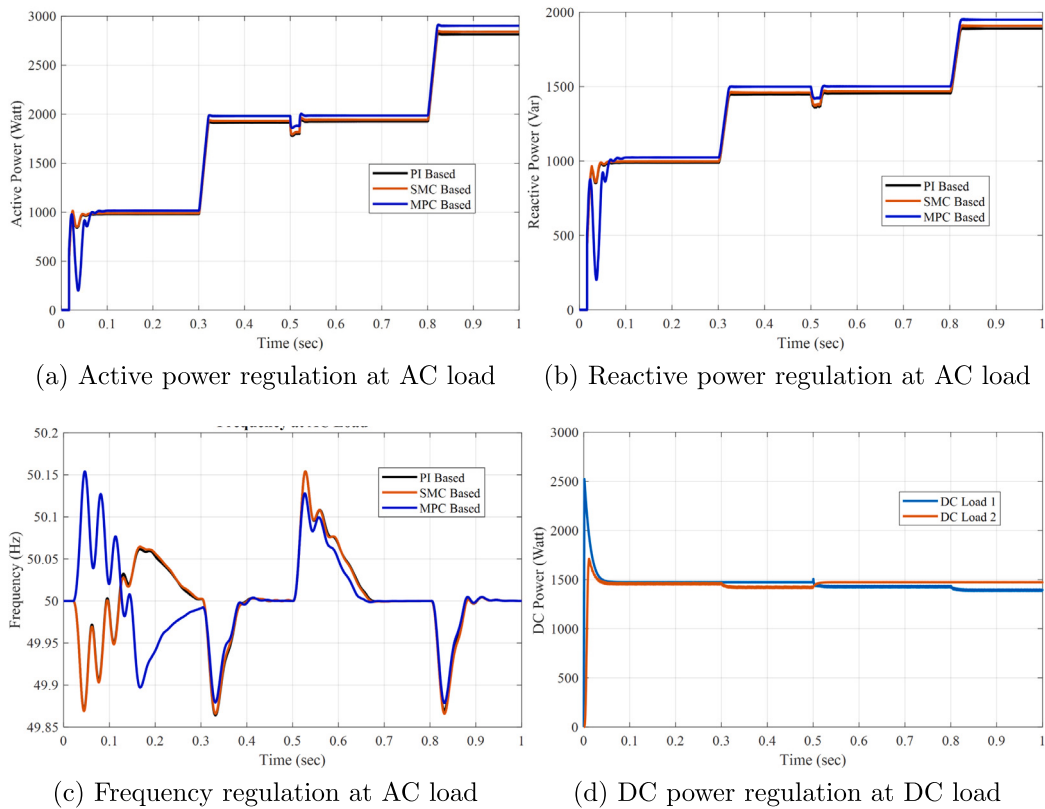


Fig. 7. Case 2 : Power flowing with AC load increments & MG transitions.

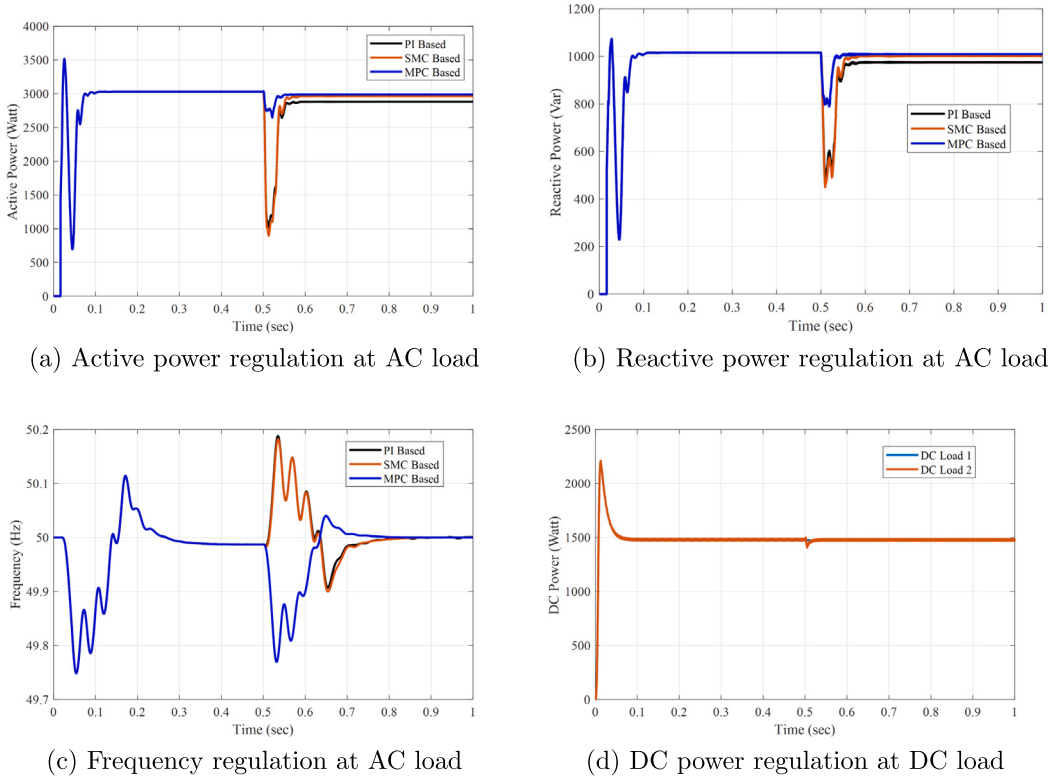


Fig. 8. Case 3 : Power flow from grid connected to islanded mode.

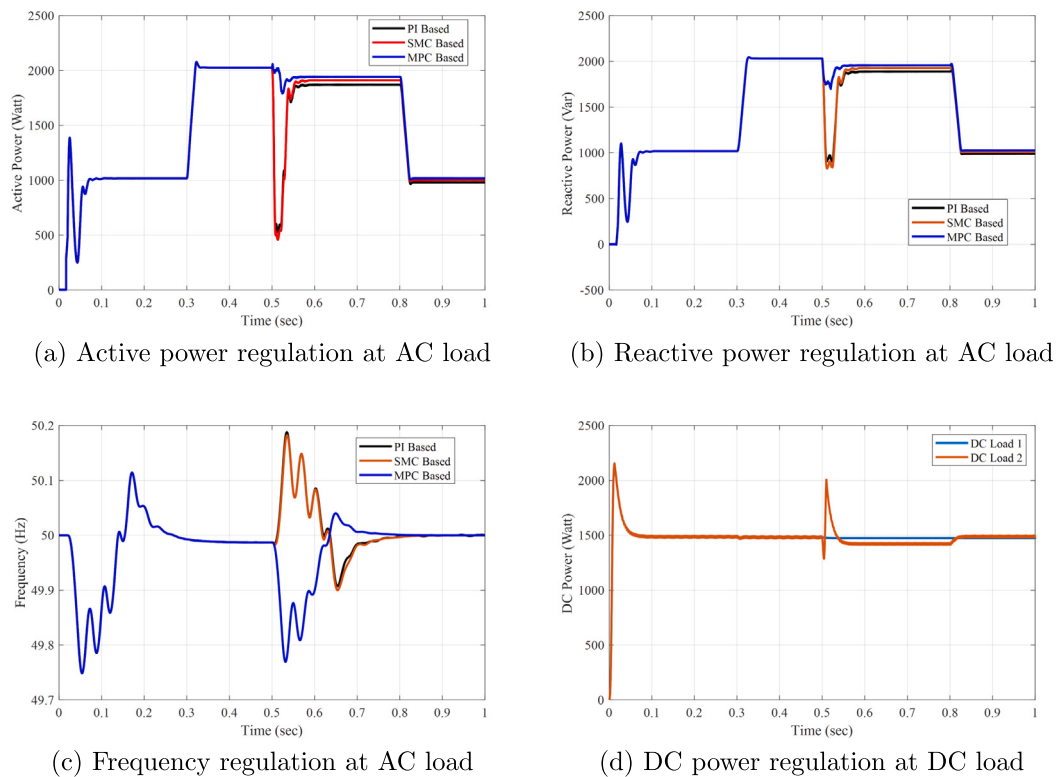


Fig. 9. Case 4 : Power flow from grid connected to islanded mode with load variations.

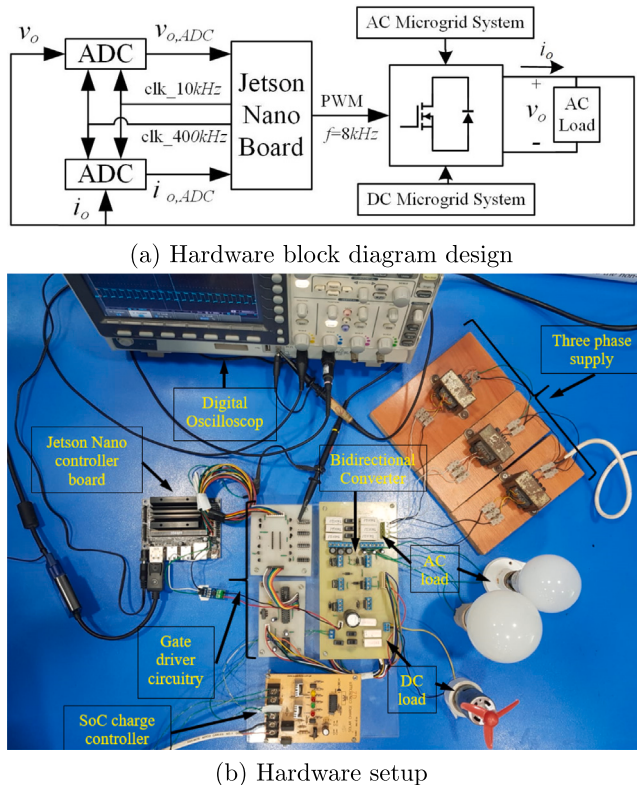


Fig. 10. Hardware implementations.

in the plot. Subsequently, the main grid is disconnected at $t = 0.5$ s. Now, the power demand needs to be fulfilled within the microgrids. Therefore, MG1 starts providing the power to both the MG1 and MG2 without the interception. In this case, we observed the performance of the proposed MPC-based secondary control is significantly better than that of the conventional controllers. At $t > 0.5$ s, the load power is precisely regulated at 2 kW load demand when using the MPC-based controller. Consequently, the dip in load power amounts to $\Delta P_{load}^{MPC} = 150$ W and $\Delta P_{load}^{PI,SMC} = 1520$ W. Lastly, the 1 kW load removed at $t = 0.8$ s which can be seen in plot.

Fig. 9(b) shows the reactive power variations during the microgrid transitions. Here, we can observe that the performance of reactive power by applying MPC based secondary controller is optimal as compared to the other controllers. The reactive power variation can be measured for proposed and conventional controllers are $\Delta P_{load}^{MPC} = 470$ VAR and $\Delta P_{load}^{PI,SMC} \approx 1150$ VAR.

In **Fig. 9(c)**, a comparison is made between conventional and proposed secondary controllers, focusing on frequency variations resulting from microgrid transition as well as load power increments. The 1 kW step load increases at $t = 0.3$ s and decreases at $t = 0.8$ s. Here, it is evident that the utilization of a secondary controller strategy leads to an enhancement in the frequency droop response, which is $\Delta f_{load}^{MPC} = 0.18$ Hz compared to $\Delta f_{load}^{PI,SMC} \approx 0.23$ Hz.

Fig. 9(d) shows the DC load power of both MG1 and MG2. We can see that both DC load of MG1 and MG2 are stable and regulated to 1.5 kW. Since MG2 supplying power $t > 0.5$ s, DC load of MG1 power drops due to load increments and grid change over, which is $\Delta P_{Dc,load1} = 0.500$ W and $\Delta P_{Dc,load2} = 0.150$ W.

7. Hardware implementations

7.1. Hardware setup

In the experimental configuration of the hybrid AC/DC shipboard microgrid, the Supervisory SMC based controller for the interlinking

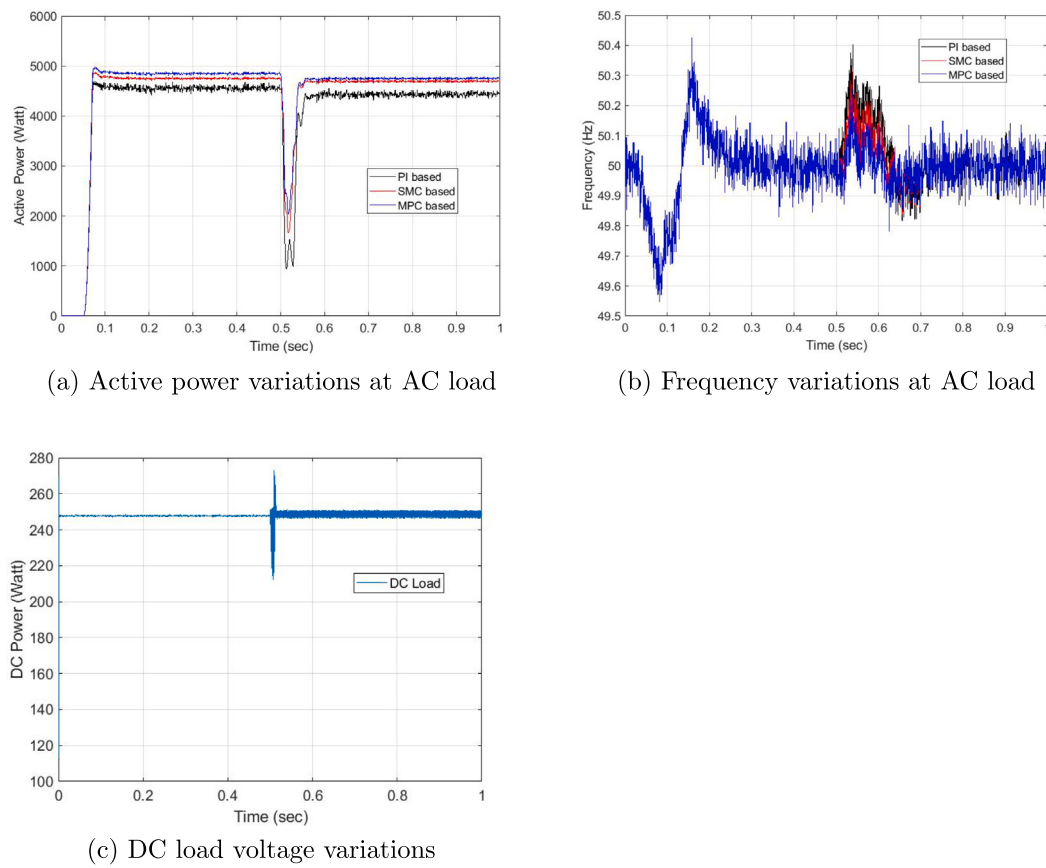


Fig. 11. Scenario 1 : Practical results of power flow from AC to DC side then DC to AC side comparisons.

converter is implemented on a Jetson Nano board, chosen for its robust computing capabilities in a compact, low-power package. With a quad-core ARM Cortex-A57 CPU and an NVIDIA Maxwell GPU featuring 128 CUDA cores (Orouzoglou, 2018), the Jetson Nano provides ample processing power to support real-time control, Hardware In the Loop (HIL) simulations, complex control algorithms, and optimization routines necessary for supervisory control within a hybrid shipboard microgrid (Gozuoglu et al., 2024).

Control algorithms, including hierarchical control schemes and a supervisory model predictive controller, are deployed on the Jetson Nano using languages like Python and C/C++. The board's compatibility with widely used frameworks such as TensorFlow and PyTorch facilitates the integration of sophisticated control algorithms, machine learning models, and optimization techniques. Communication with other shipboard microgrid components, such as power converters, energy storage units, and external controllers, is established by multiple protocols, including Ethernet, CAN bus, and serial communication. This broad protocol support enables efficient coordination of diverse components within the microgrid.

The Jetson Nano orchestrates power flow between the AC and DC segments of the shipboard microgrid, managing the bidirectional IC using HIL to enable real-time controlling. By regulating the converter operations based on supervisory control actions, the Jetson Nano ensures balanced power distribution and optimized energy management. Therefore, it supports system stability and reliability. Fig. 10a illustrates the hardware implementation block diagram. Fig. 10b shows the practical setup for the hybrid SMG.

7.2. Hardware results

A comparative analysis of hardware results for PI, SMC and MPC control schemes within the shipboard microgrid setup is presented in Figs. 11 and 12.

7.2.1. Scenario 1 : Power flow from AC to DC side then DC to AC side

In Fig. 11(a), grid transition scenario 1 is demonstrated, where power initially flows from the AC side to the DC side. At $t = 0.5$ s, the power direction reverses from DC to AC, with a power deviation of $\Delta P_{droop} = 1$ kW. Here, we observed that SMC has better performance as compare to both the PI and SMC control schemes.

Fig. 11(b) compares frequency variations induced by microgrid switching between the conventional control method and the proposed secondary controller approach, highlighting the performance improvements of the proposed method.

Fig. 11(c) shows the DC load waveform, which is regulated to $P_{DC,L} = 250$ W load receives power from the AC source initially, during $0 \text{ s} < t \leq 0.5 \text{ s}$ after which it transitions to DC source power. Harmonics introduced by inverter switching in the IC are also noted in this scenario.

7.2.2. Scenario 2 : Power flow from DC to AC side then AC to DC side

Fig. 12(a) illustrates grid transition scenario 2, where power initially flows from DC to AC, then switches to AC to DC at $t = 0.5$ s, AC to DC side with identical load increments at $t = 0.3$ s and $t = 0.7$ s. Here, we observed that the $\Delta P_{droop} = 1$ kW. Here, we observed that SMC has better performance as compare to both the PI and SMC control schemes.

Frequency variations due to microgrid switching are again compared in Fig. 12(b), showcasing differences between the conventional control and the secondary controller-based method.

Finally, Fig. 12(c) presents the DC load waveform regulated to $P_{DC,L} = 250$ W. Identical step DC load increased at $t = 0.3$ s and $t = 0.7$ s. Afterward, the DC load stabilizes, drawing power from the AC source. Harmonics due to the inverter switching in the IC are also observed in this configuration. By comparing the practical results and performances we conclude that the proposed MPC based controller has the optimal performance than PI and SMC based hierarchical control designs.

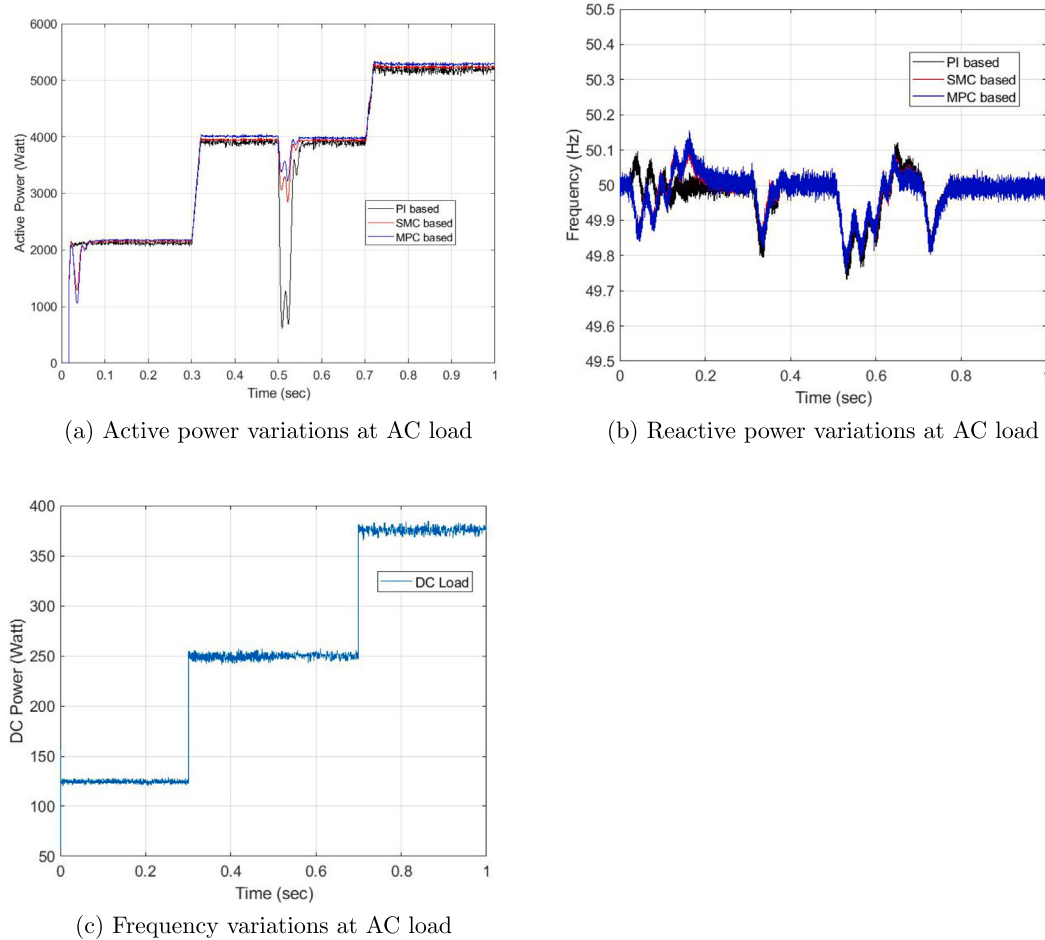


Fig. 12. Scenario 2 : Practical results of power flow from DC to AC side then AC to DC side comparisons.

8. Conclusions

This paper compares the output responses from hierarchical secondary controllers within hybrid AC/DC shipboard microgrids. The model operates secondary control. In addition to representing the attributes of the IC responsible for power interchange between AC/DC microgrid units, the model also delineates the fundamental behavior of AC/DC microgrid control. In order to evaluate the precision of the proposed model and to verify its performance, simulation tests were done using different cases of real SMGs.

The simulation results show that the developed MPC achieves far better performance compared to the traditional PI and SMC controllers for mitigating non-linearity and achieving stability in facing static and dynamic loads. In particular, by comparing the performance of the proposed controller, the SMC improved the active and reactive power droop control by about 27.8% over the conventional PI controller. Moreover, the MPC improved further the transient response, energy efficiency, and fault tolerance.

Furthermore, the literature reviews were accompanied by hardware implementation and validation steps to prove the feasibility of the proposed control schemes and show a 33.5% improvement in power droop. The foregoing hardware results support the simulation outcomes, especially regarding improvement in voltage stability and light bidirectional power transfer. Therefore, the proposed approach can be considered effective and reliable in supporting the bidirectional power flow in the hybrid shipboard microgrids.

CRediT authorship contribution statement

Farooq Alam: Writing – original draft, Software, Investigation, Formal analysis, Conceptualization. **Sajjad Haider Zaidi:** Validation, Supervision, Methodology. **Arsalan Rehmat:** Writing – review & editing, Resources, Data curation. **Bilal M. Khan:** Visualization, Software, Resources, Project administration.

Declaration of competing interest

The authors declare that they have no known competing financial interests or personal relationships that could have appeared to influence the work reported in this paper.

Data availability

The data that has been used is confidential.

References

- Aghdam, M.M., Li, L., Zhu, J., 2020. Comprehensive study of finite control set model predictive control algorithms for power converter control in microgrids. *IET Smart Grid* 3 (1), 1–10.
- Alam, F., Ashfaq, M., Zaidi, S.S., Memon, A.Y., 2016. Robust droop control design for a hybrid AC/DC microgrid. In: 2016 UKACC 11th International Conference on Control. IEEE, pp. 1–6.
- Alam, F., Haider Zaidi, S.S., Rehmat, A., Mutarraf, M.U., Nasir, M., Guerrero, J.M., 2022. Robust hierarchical control design for the power sharing in hybrid shipboard microgrids. *Inventions* 8 (1), 7.

- Alsmeier, H., Savchenko, A., Findeisen, R., 2024. Neural horizon model predictive control—Increasing computational efficiency with neural networks. arXiv preprint arXiv:2408.09781.
- Ansari, S., Chandel, A., Tariq, M., 2020. A comprehensive review on power converters control and control strategies of AC/DC microgrid. *IEEE Access* 9, 17998–18015.
- Azeem, O., Ali, M., Abbas, G., Uzair, M., Qahmash, A., Algarni, A., Hussain, M.R., 2021. A comprehensive review on integration challenges, optimization techniques and control strategies of hybrid AC/DC microgrid. *Appl. Sci.* 11 (14), 6242.
- Babayomi, O., Li, Y., Zhang, Z., Kennel, R., Kang, J., 2020. Overview of model predictive control of converters for islanded AC microgrids. In: 2020 IEEE 9th International Power Electronics and Motion Control Conference (IPEMC2020-ECCE Asia). IEEE, pp. 1023–1028.
- Bernardino, L.F., Skogestad, S., 2024. Optimal switching of MPC cost function for changing active constraints. *J. Process Control* 142, 103298.
- Bharatee, A., Ray, P.K., Subudhi, B., Ghosh, A., 2022. Power management strategies in a hybrid energy storage system integrated AC/DC microgrid: A review. *Energies* 15 (19), 7176. <http://dx.doi.org/10.3390/en15197176>.
- Bledt, G., 2020. Regularized Predictive Control Framework for Robust Dynamic Legged Locomotion (Ph.D. thesis). Massachusetts Institute of Technology.
- Chen, J., Chen, Y., Tong, L., Peng, L., Kang, Y., 2020. A backpropagation neural network-based explicit model predictive control for DC–DC converters with high switching frequency. *IEEE J. Emerg. Sel. Top. Power Electron.* 8 (3), 2124–2142. <http://dx.doi.org/10.1109/JESTPE.2020.2968475>.
- Chen, Z., Lai, J., Li, P., Awad, O.I., Zhu, Y., 2024. Prediction horizon-varying model predictive control (MPC) for autonomous vehicle control. *Electronics* 13 (8), 1442.
- Clarke, W.C., Manzie, C., Bear, M.J., 2016. An economic MPC approach to microgrid control. In: 2016 Australian Control Conference (AuCC). pp. 276–281. <http://dx.doi.org/10.1109/AUCC.2016.7868202>.
- Cortes, P., Rodriguez, J., Silva, C., Flores, A., 2012. Delay compensation in model predictive current control of a three-phase inverter. *IEEE Trans. Ind. Electron.* 59 (2), 1323–1325. <http://dx.doi.org/10.1109/TIE.2011.2157284>.
- Dahane, A.S., Sharma, R.B., 2024. Hybrid AC-DC microgrid coordinated control strategies: A systematic review and future prospect. *Renew. Energy Focus* 100553.
- Ding, B., Yang, Y., 2024. Model Predictive Control. John Wiley & Sons.
- Eghatelpour, N., Farjah, E., 2014. Power control and management in a hybrid AC/DC microgrid. *IEEE Trans. Smart Grid* 5 (3), 1494–1505.
- Elnawawi, S., Siang, L.C., O'Connor, D.L., Gopaluni, R.B., 2022. Interactive visualization for diagnosis of industrial model predictive controllers with steady-state optimizers. *Control Eng. Pract.* 121, 105056.
- Esfahani, H.N., Velni, J.M., 2024. Cooperative multi-agent Q-learning using distributed MPC. *IEEE Control. Syst. Lett.*
- Espina, E., Cárdenas, R., Donoso, F., Urrutia, M., Espinoza, M., 2019. A novel distributed secondary control strategy applied to hybrid AC/DC microgrids. In: 2019 21st European Conference on Power Electronics and Applications (EPE'19 ECCE Europe). IEEE, pp. P-1.
- Fang, S., Xu, Y., Li, Z., Zhao, T., Wang, H., 2019. Two-step multi-objective management of hybrid energy storage system in all-electric ship microgrids. *IEEE Trans. Veh. Technol.* 68 (4), 3361–3373.
- Garcia-Torres, F., Bordons, C., Ridao, M.A., 2019. Optimal economic schedule for a network of microgrids with hybrid energy storage system using distributed model predictive control. *IEEE Trans. Ind. Electron.* 66 (3), 1919–1929. <http://dx.doi.org/10.1109/TIE.2018.2826476>.
- Gozuoglu, A., Ozgonenel, O., Gezegin, C., 2024. CNN-LSTM based deep learning application on jetson nano: Estimating electrical energy consumption for future smart homes. *Int. Things* 101148.
- Hosseinzadeh, M., Salmasi, F.R., 2015. Robust optimal power management system for a hybrid AC/DC micro-grid. *IEEE Trans. Sustain. Energy* 6 (3), 675–687. <http://dx.doi.org/10.1109/tste.2015.2405935>.
- Hou, J., Song, Z., Hofmann, H., Sun, J., 2019. Adaptive model predictive control for hybrid energy storage management in all-electric ship microgrids. *Energy Convers. Manage.* 198, 111929.
- Hou, J., Song, Z., Hofmann, H.F., Sun, J., 2020. Control strategy for battery/flywheel hybrid energy storage in electric shipboard microgrids. *IEEE Trans. Ind. Informatics* 17 (2), 1089–1099.
- Huang, W., Qahouq, J.A.A., 2014. Energy sharing control scheme for state-of-charge balancing of distributed battery energy storage system. *IEEE Trans. Ind. Electron.* 62 (5), 2764–2776.
- Jain, A., 2020. Methods for Data-Driven Model Predictive Control (Ph.D. thesis). University of Pennsylvania.
- Jena, S., Padhy, N.P., 2020. Distributed cooperative control for autonomous hybrid AC/DC microgrid clusters interconnected via back-to-back converter control. In: 2020 IEEE Power & Energy Society General Meeting. PESGM, IEEE, pp. 1–5.
- Jia, Y., Dong, Z.Y., Sun, C., Chen, G., 2020. Distributed economic model predictive control for a wind–photovoltaic–battery microgrid power system. *IEEE Trans. Sustain. Energy* 11 (2), 1089–1099. <http://dx.doi.org/10.1109/TSTE.2019.2919499>.
- Jianfang, X., Peng, W., Setyawati, L., Chi, J., Hoong, C.F., 2015. Energy management system for control of hybrid AC/DC microgrids. In: 2015 IEEE 10th Conference on Industrial Electronics and Applications. ICIEA, IEEE, pp. 778–783.
- Jin, H., Yang, X., 2023. Bilevel optimal sizing and operation method of fuel cell/battery hybrid all-electric shipboard microgrid. *Mathematics* 11 (12), 2728.
- Jithin, S., Rajeev, T., 2022. Novel adaptive power management strategy for hybrid AC/DC microgrids with hybrid energy storage systems. *J. Power Electron.* 22 (12), 2056–2068. <http://dx.doi.org/10.1007/s43236-022-00506-x>.
- Judewicz, M.G., González, S.A., Fischer, J.R., Martínez, J.F., Carrica, D.O., 2018. Inverter-side current control of grid-connected voltage source inverters with LCL filter based on generalized predictive control. *IEEE J. Emerg. Sel. Top. Power Electron.* 6 (4), 1732–1743. <http://dx.doi.org/10.1109/JESTPE.2018.2826365>.
- Karnavas, Y.L., Nivolianiti, E., 2023. Optimal load frequency control of a hybrid electric shipboard microgrid using jellyfish search optimization algorithm. *Appl. Sci.* 13 (10), 6128.
- Khooban, M.-H., Dragicevic, T., Blaabjerg, F., Delimar, M., 2017. Shipboard microgrids: A novel approach to load frequency control. *IEEE Trans. Sustain. Energy* 9 (2), 843–852.
- Kou, P., Liang, D., Gao, L., 2017. Distributed coordination of multiple PMGs in an islanded DC microgrid for load sharing. *IEEE Trans. Energy Convers.* 32 (2), 471–485. <http://dx.doi.org/10.1109/TEC.2017.2649526>.
- Lee, H.-J., Vu, B.H., Zafar, R., Hwang, S.-W., Chung, I.-Y., 2021. Design framework of a stand-alone microgrid considering power system performance and economic efficiency. *Energies* 14 (2), 457.
- Lima, D.M., Montagner, V.F., Maccari, L.A., 2017. Generalized predictive control with harmonic rejection applied to a grid-connected inverter with LCL filter. In: 2017 Brazilian Power Electronics Conference. COBEP, pp. 1–6. <http://dx.doi.org/10.1109/COBEP.2017.8257372>.
- Liu, K., Liu, T., Tang, Z., Hill, D.J., 2019. Distributed MPC-based frequency control in networked microgrids with voltage constraints. *IEEE Trans. Smart Grid* 10 (6), 6343–6354. <http://dx.doi.org/10.1109/TSG.2019.2902595>.
- Liu, S., Wang, X., Liu, P.X., 2015. Impact of communication delays on secondary frequency control in an islanded microgrid. *IEEE Trans. Ind. Electron.* 62 (4), 2021–2031. <http://dx.doi.org/10.1109/TIE.2014.2367456>.
- Lou, G., Gu, W., Xu, Y., Cheng, M., Liu, W., 2017. Distributed MPC-based secondary voltage control scheme for autonomous droop-controlled microgrids. *IEEE Trans. Sustain. Energy* 8 (2), 792–804. <http://dx.doi.org/10.1109/TSTE.2016.2620283>.
- Lu, P., Zhang, N., Ye, L., Du, E., Kang, C., 2024. Advances in model predictive control for large-scale wind power integration in power systems: A comprehensive review. *Adv. Appl. Energy* 100177.
- Ma, A., Liu, K., Zhang, Q., Liu, T., Xia, Y., 2020. Event-triggered distributed MPC with variable prediction horizon. *IEEE Trans. Autom. Control* 66 (10), 4873–4880.
- MacKinnon, L., Ramesh, P.S., Mhaskar, P., Swartz, C.L., 2022. Dynamic real-time optimization for nonlinear systems with Lyapunov stabilizing MPC. *J. Process Control* 114, 1–15.
- Majumder, R., Chaudhuri, B., Ghosh, A., Majumder, R., Ledwich, G., Zare, F., 2009. Improvement of stability and load sharing in an autonomous microgrid using supplementary droop control loop. *IEEE Trans. Power Syst.* 25 (2), 796–808.
- Marimuthu, R., et al., 2023. Review on advanced control techniques for microgrids. *Energy Rep.* 10, 3054–3072.
- Mariscotti, A., 2021. Power quality phenomena, standards, and proposed metrics for dc grids. *Energies* 14 (20), 6453.
- Morstyn, T., Hredzak, B., Agelidis, V.G., 2016. Dynamic optimal power flow for DC microgrids with distributed battery energy storage systems. In: 2016 IEEE Energy Conversion Congress and Exposition. ECCE, pp. 1–6. <http://dx.doi.org/10.1109/ECCE.2016.7855059>.
- Morstyn, T., Hredzak, B., Aguilera, R.P., Agelidis, V.G., 2018. Model predictive control for distributed microgrid battery energy storage systems. *IEEE Trans. Control Syst. Technol.* 26 (3), 1107–1114. <http://dx.doi.org/10.1109/TCST.2017.2699159>.
- Mosayebi, M., Sadeghzadeh, S.M., Gheisarnejad, M., Khooban, M.H., 2020. Intelligent and fast model-free sliding mode control for shipboard DC microgrids. *IEEE Trans. Transp. Electrification* 7 (3), 1662–1671.
- Mutarraf, M.U., Guan, Y., Terriche, Y., Su, C.-L., Nasir, M., Vasquez, J.C., Guerrero, J.M., 2022. Adaptive power management of hierarchical controlled hybrid shipboard microgrids. *IEEE Access* 10, 21397–21411.
- Mutarraf, M.U., Terriche, Y., Nasir, M., Niazi, K.A.K., Vasquez, J.C., Guerrero, J.M., 2019. Hybrid energy storage systems for voltage stabilization in shipboard microgrids. In: 2019 9th International Conference on Power and Energy Systems. ICPES, IEEE, pp. 1–6.
- Mutarraf, M.U., Terriche, Y., Niazi, K.A.K., Vasquez, J.C., Guerrero, J.M., 2018. Energy storage systems for shipboard microgrids—A review. *Energies* 11 (12), 3492.
- Nassourou, M., Puig, V., Blesa, J., Ocampo-Martinez, C., 2017. Economic model predictive control for energy dispatch of a smart micro-grid system. In: 2017 4th International Conference on Control, Decision and Information Technologies (CoDIT), pp. 0944–0949. <http://dx.doi.org/10.1109/CoDIT.2017.8102719>.
- Nejabatkhan, F., Li, Y.W., 2014. Overview of power management strategies of hybrid AC/DC microgrid. *IEEE Trans. Power Electron.* 30 (12), 7072–7089.
- Nguyen, H.T., Jung, J.-W., 2018. Finite control set model predictive control to guarantee stability and robustness for surface-mounted PM synchronous motors. *IEEE Trans. Ind. Electron.* 65 (11), 8510–8519. <http://dx.doi.org/10.1109/TIE.2018.2814006>.
- Nguyen, T.-T., Yoo, H.-J., Kim, H.-M., 2018. Model predictive control of inverters in microgrid with constant switching frequency for circulating current suppression. In: TENCON 2018 - 2018 IEEE Region 10 Conference. pp. 1566–1571. <http://dx.doi.org/10.1109/TENCON.2018.8650549>.

- Ni, F., Zheng, Z., Xie, Q., Xiao, X., Zong, Y., Huang, C., 2021. Enhancing resilience of DC microgrids with model predictive control based hybrid energy storage system. *Int. J. Electr. Power Energy Syst.* 128, 106738.
- Orlitzoglou, I., 2018. Design and implementation of image processing algorithms on embedded CPU-GPU-SoC devices.
- Roy, S.P., Shubham, Singh, A., Roy, O., 2023. MPC-based frequency regulation for shipboard microgrid. In: International Symposium on Sustainable Energy and Technological Advancements. Springer, pp. 25–33.
- Sachs, J., Sawodny, O., 2016. A two-stage model predictive control strategy for economic diesel-PV-battery island microgrid operation in rural areas. *IEEE Trans. Sustain. Energy* 7 (3), 903–913. <http://dx.doi.org/10.1109/TSTE.2015.2509031>.
- Sahoo, B., Routray, S.K., Rout, P.K., 2021. AC, DC, and hybrid control strategies for smart microgrid application: A review. *Int. Trans. Electr. Energy Syst.* 31 (1), e12683.
- Varvaros, S., Kirli, D., Merlin, M.M., Kiprakis, A.E., 2022. Major challenges towards energy management and power sharing in a hybrid AC/DC microgrid: a review. *Energies* 15 (23), 8851.
- Shagar, V., Jayasinghe, S.G., Enshaei, H., 2017. Effect of load changes on hybrid shipboard power systems and energy storage as a potential solution: A review. *Inventions* 2 (3), 21.
- Taher, A.M., Hasanien, H.M., Ginidi, A.R., Taha, A.T., 2021. Hierarchical model predictive control for performance enhancement of autonomous microgrids. *Ain Shams Eng. J.* 12 (2), 1867–1881.
- Tian, W., Liu, L., Zhang, X., Shao, J., Ge, J., 2024. Adaptive hierarchical energy management strategy for fuel cell/battery hybrid electric UAVs. *Aerospace Sci. Technol.* 146, 108938.
- Verheijen, P., Derkani, A., Agarwal, Y., Lazar, M., Goswami, D., 2024. Multilevel parallel GPU implementation of SQP solvers for nonlinear MPC. In: 2024 European Control Conference ECC, IEEE, pp. 2292–2298.
- Wang, J., Tang, Y., Lin, P., Liu, X., Pou, J., 2020a. Deadbeat predictive current control for modular multilevel converters with enhanced steady-state performance and stability. *IEEE Trans. Power Electron.* 35 (7), 6878–6894. <http://dx.doi.org/10.1109/TPEL.2019.2955485>.
- Wang, G., Wang, X., Wang, F., Han, Z., 2020b. Research on hierarchical control strategy of AC/DC hybrid microgrid based on power coordination control. *Appl. Sci.* 10 (21), 7603.
- Xie, H., Dai, L., Lu, Y., Xia, Y., 2021a. Disturbance rejection MPC framework for input-affine nonlinear systems. *IEEE Trans. Autom. Control* 67 (12), 6595–6610.
- Xie, H., Dai, L., Luo, Y., Xia, Y., 2021b. Robust MPC for disturbed nonlinear discrete-time systems via a composite self-triggered scheme. *Automatica* 127, 109499.
- Xie, P., Guerrero, J.M., Tan, S., Bazmohammadi, N., Vasquez, J.C., Mehrzadi, M., Al-Turki, Y., 2021c. Optimization-based power and energy management system in shipboard microgrid: A review. *IEEE Syst. J.*
- Yamashita, D.Y., Vechiu, I., Gaubert, J.-P., 2021. Two-level hierarchical model predictive control with an optimised cost function for energy management in building microgrids. *Appl. Energy* 285, 116420.
- Yang, X., He, H., Zhang, Y., Chen, Y., Weng, G., 2019. Interactive energy management for enhancing power balances in multi-microgrids. *IEEE Trans. Smart Grid* 10 (6), 6055–6069. <http://dx.doi.org/10.1109/TSG.2019.2896182>.
- Yfantis, V., 2024. Distributed Optimization of Constraint-Coupled Systems via Approximations of the Dual Function (Ph.D. thesis). Rheinland-Pfälzische Technische Universität Kaiserslautern-Landau.
- Yoo, H.-J., Nguyen, T.-T., Kim, H.-M., 2019. Consensus-based distributed coordination control of hybrid AC/DC microgrids. *IEEE Trans. Sustain. Energy* 11 (2), 629–639.
- Zafari, A., Mehrasa, M., Rouzbeh, K., Sadabadi, M.S., Bacha, S., Hably, A., 2020. DC-link voltage stability-based control strategy for grid-connected hybrid AC/DC microgrid. In: 2020 2nd Global Power, Energy and Communication Conference. GPECOM, IEEE, pp. 268–273.
- Zhang, Z., Babayomi, O., Dragicevic, T., Heydari, R., Garcia, C., Rodriguez, J., Kennel, R., 2022. Advances and opportunities in the model predictive control of microgrids: Part I-primary layer. *Int. J. Electr. Power Energy Syst.* 134, 107411.
- Zhaoxia, X., Tianli, Z., Huaimin, L., Guerrero, J.M., Su, C.-L., Vásquez, J.C., 2019. Coordinated control of a hybrid-electric-ferry shipboard microgrid. *IEEE Trans. Transp. Electrification* 5 (3), 828–839.
- Zheng, Y., Li, S., Tan, R., 2018. Distributed model predictive control for on-connected microgrid power management. *IEEE Trans. Control Syst. Technol.* 26 (3), 1028–1039. <http://dx.doi.org/10.1109/TCST.2017.2692739>.
- Zhuoyu, G., Shaoyuan, L., Yi, Z., 2017. Distributed model predictive control for secondary voltage of the inverter-based microgrid. In: 2017 36th Chinese Control Conference. CCC, pp. 4630–4634. <http://dx.doi.org/10.23919/ChiCC.2017.8028085>.
- Zolfaghari, M., Gharehpetian, G.B., Shafie-khah, M., Catalão, J.P., 2022. Comprehensive review on the strategies for controlling the interconnection of AC and DC microgrids. *Int. J. Electr. Power Energy Syst.* 136, 107742.